CHAPTER ONE

INTRODUCTION

1.1 Background

Carbon nanotubes (CNTs) are wires of pure carbon which its graphite sheets being rolling up into a cylinder. CNTs can be categorized according to their crystalline and amorphous structures. Commonly, CNTs are classified into single-walled carbon nanotubes (SWCNTs) which consist of one cylinder and multi-walled carbon nanotubes (MWCNTs) comprising an array on tubes being concentrically nested (Takeshi *et al*, 2010). All crystalline CNTs can be represented by a pair of indices (*n*, *m*) called the chiral vector. In contrast, the amorphous carbon nanotubes (α-CNTs) possess high degree of disorder structures due to defects at the amorphous wall. As a result, any possible problem due to chirality is absence for α-CNTs (Rakitin *et al*, 2000).

Since the discovery of CNTs, by Iijima (1991), it has attracted worldwide attention due to their interesting properties and various potential applications. CNTs exhibitan extraordinary strength, excellent electrical properties and efficient thermal conductivity which suit them to a tremendously diverse range of applications such as sensors, probes, lithium batteries, gas adsorption, hydrogen storage and others (Meyyappan, 2005; O'Connell, 2006; Peter, 2009). Interestingly, the CNTs have been applied in field emission display devices as cathode-ray tube-type lighting elements and

vacuum-fluorescence display panels (Saito *et al*, 2000). However, crystalline CNTs pose a challenge for synthesizing its in a large quantity due to its very critical deposition conditions like high temperature, various catalyst supports, complicated steps to process, expensive cost, etc(Wang *et al*, 2005). Hence, efforts were made to develop simpler synthesis routes for synthesizing novel CNTs in a large scale.

In that light, amorphous carbon nanotubes (α-CNTs) are constantly gaining importance due to its simple synthesis conditions (Jha *et al*, 2009). Moreover, α-CNTs have also created strong interest due to their defects at the amorphous wall. As their diameter in the nanometer range with high surface area, α-CNTs can be used for the development of new potential nanodevices, like gaseous adsorbent and catalyst support (Nishinoa *et al*,2003; Xiong *et al*, 2004; Liu *et al*,2007; Luo *et al*, 2006).

However, there are some difficulties in producing the pure CNTs as the as-prepared CNTs are usually accompanied by metallic impurities or carbonaceous. The presence of trace amount of iron in the as-prepared CNTs can be removed by washing it with the diluted hydrochloric acid (HCl) and deionized water (Jha, 2011). Therefore, purification process is important in producing pure CNTs since the defects may affect their properties.

In recent years, there are strong attentions to hybrid α-CNTs with inorganic materials because of their outstanding properties and significant potential applications.

Researchers are focusing on a new type of hybrid material such as CNT- inorganic hybrid, that replace the organic compound within the CNT (Dominik, 2010).

The goal of this work is to develop hybrid materials of cuprous (Cu_2O) with α-CNTs. Cuprous has gained increasing attention because of its p-type semiconducting nature with distinctive properties, which makes it suitable for applications in gas sensors, photo catalysts, and electrochemical sensors (Rajendra *et al*, 2011).

In this work, the α-CNTs were synthesized by using a simple chemical route at a low temperature and pressure conditions with a short processing period. Then,the as-synthesized CNTs were purified with HCl and deionized water for removing all the trace elements. Finally, hybrid of α-CNTs-Cu_2O were prepared through mixing, stirring and dehydrating processes. Samples were then characterized by Field Emission Scanning Electron Microscopy (FESEM), Transmission Electron Microscopy (TEM), X-ray analysis (EDX), UV-Vis spectroscopy and Raman spectroscopy. The surface texture, morphological, studies of the samples were performed by Field Emission Scanning Electron Microscopy (FESEM) and Transmission Electron Microscopy (TEM). The elemental composition of the carbon nanotubes were identified by energy dispersive X-ray analysis (EDX). The optical properties of the samples were performed using UV-visible spectroscopy and Raman spectroscopy.

1.2 Important Research Problems

Carbon nanotubes have attracted much attention because of their many potential applications. However, the problem arise because the synthesis of CNT is not easy as it requires high temperature, catalyst support and expensive cost (Wang et al, 2005a; Wang et al, 2005b). Therefore, synthesizing the amorphous carbon nanotubes α-CNTs come into the picture. Even though the synthesis process is relatively simple, the α-CNTs typically will be contaminated with metal oxides which lead to impurities. Therefore the purification process was essential to produce a pure of α-CNT. Enhancement of the properties of CNT through hybridization with other materials is an important issue. In this work, hybridization between α-CNTs and Cu_2O was conducted. The unique properties of Cu_2O may enhance the property of the α-CNT-Cu_2O hybrid material.

1.3 Research Objectives

The main objectives of this project are as follows:

1) To synthesize the amorphous carbon nanotubes (α-CNTs) through chemical route.

2) To hybridize the α-CNTs with Cu_2O for the enhancement of the optical properties.

3) To characterize the α-CNT and hybrid α-CNTs–Cu_2O via Transmission Electron Microscopy (TEM), Field Emission Scanning Electron Microscopy (FE-SEM), X-ray Diffraction (XRD), Energy-Dispersive X-ray (EDX), Raman Spectroscopy and Ultraviolet-Visible (UV-Vis) spectrophotometer.

1.4 Scope of Work

In this work, α-CNTs were synthesized using a relatively simple technique that only required a low temperature and pressure conditions in a short processing period. Precursor materials were heated inside a furnace. Untreated, treated and hybridized sample were prepared. Firstly, the as-prepared α-CNTs (untreated sample) were synthesized at 230°C. It was purified with diluted hydrochloric acid (HCl) and deionized water to obtain a purified α-CNT and named as treated sample. Finally, the treated samples were hybridized with Cu_2O to produce α-CNTs-Cu_2O sample.

The morphological, microstructural, elemental and optical studies were conducted for all samples. Instruments such as field emissions canning electron microscope (FE-SEM), transmission electron microscope (TEM), X-ray diffraction (XRD) spectrometer, and energy-dispersive X-ray (EDX) spectrometer were utilized. Ultraviolet-visible (UV-Vis) and Raman spectroscopy studies were conducted to examine optical features of CNT.

Chapter Two

Literature Review

2.1 Historical Developments

The discovery that carbon could form stable and ordered structures other than graphite and diamond stimulated researchers worldwide to search other new forms of carbon (MacKenzie *et al*, 2009). Interest in carbon nanotubes (CNTs) was a direct consequence of the synthesis of Buckminster fullerene, C_{60}, and other type of fullerenes in 1985. New impetus was generated to this search as C_{60} was synthesized in a simple arc-evaporation apparatus by the Japanese scientist Sumio Iijima in 1991 (Iijima, 1991).

The tubes were discovered to contain at least two layers and ranged in outer diameter from about 3 to 30 nm known as multi-walled carbon nanotubes (MWCNTs).In 1993, a new class of CNT, which is single-walled carbon nanotubes (SWCNTs) were discovered, with a single graphite layer (Bethune *et al*, 1993*;* Ajayan, 1999).

These SWCNTs were generally narrower than the MWCNTs, with diameters typically in the range of 1 to 2 nm.Double-walled carbon nanotubes (DWCNTs) were then developed by the arc discharge technique with a mixture of different catalysts with

the outer and inner diameter in the range of 1.9 nm – 5 nm and 1.1 nm – 4.2 nm, respectively (Hutchison *et al*, 2001). Another type of nanotubes with highly disordered structure called as amorphous carbon nanotubes (α-CNTs) were produced successfully for the first time in 2001 via the CVD process (Ci *et al*, 2001). The works on α-CNTs is continually growth from this.

2.2 Type of Carbon Nanotubes (CNTs)

The structures of CNTs made up of rolled sheets of graphite. CNTs are classified as either single-walled (SWCNTs) or multi-walled nanotubes (MWCNTs). Their properties are a mix of diamond and graphite with a strong, thermally conductive like diamond and electrically conductive like graphite. Depending on their chirality, CNTs can be either metallic or semi-conducting. The physical properties of CNTs are, in the typical diameter of 1 – 140 nm and lengths in the micrometer scale, and also have high aspect ratios (Vikas, 2010). All the crystalline CNTs, like SWCNTs, DWCNTs and MWCNTs are promising one dimensional periodic structure along the axis of the tube with extraordinary length-to-diameter ratio of up to 132,000,000:1 (Wang *et al*, 2009).

On the other hand, the chemical bonding of CNTs is constructed entirely of sp^2 bonds, similar to those of graphite. It is this bonding structure that provides unique strength to CNTs. Other types of nanotubes are amorphous carbon nanotubes (α-CNTs). α-CNT is a tubular structure made of carbon atoms, having diameter of nanometer order but length in micrometers. This type of carbon nanotube is different from crystalline CNTs. The walls of the α-CNTs are composed of many carbon clusters whose

characteristic is of short-distance order and long-distance disorder. Therefore, the properties of the α-CNTs are different from single-walled and multi-walled carbon nanotubes (Zhao *et al*, 2006).

It is well known that α-CNTs can be synthesized via some novel approaches Shih *et al* (2000) prepared vertically aligned α-CNTs on anodic alumina by using a microwave electron cyclotron resonance chemical vapor deposition (ECR-CVD) method. Ci *et al* (2003) produced α-CNTs by the floating catalyst method. Bao *et al* (2003) and Xie *et al* (2004) synthesized α-CNTs bundles by catalytic assembly of carbon rings. Nishino *et al* (2003) obtained α-CNTs from poly(tetrafluoroethylene) and ferrous chloride via chemical vapor deposition (CVD) technology at high temperatures. The types, structures, nature and historical developments of CNTs will be discussed in the following sections.

2.3 Structure and properties of Carbon Nanotubes

Diamond and graphite are the two well-known forms of crystalline carbon. Diamond has four-coordinate sp^3 carbon atoms that form an extended three-dimensional network. Graphite has three-coordinate sp^2 carbon atoms that form planar sheets. For amorphous graphite, it has random stacking of graphitic layer segments. Because of the weak interplanar interaction between two graphitic planes, these planes can move easily relative to each other, thereby forming a solid lubricant. In this sense, amorphous graphite can behave like a two-dimensional material (Saito *et al*, 1998).

The new emerging carbon allotropes, the fullerenes, are closed-cage carbon molecules with three-coordinate carbon atoms forming the spherical or nearly-spherical surfaces. However, carbon nanotubes (CNTs), which are derived from fullerenes, are the only form of carbon with extended bonding and yet with no dangling bonds (Meyyappan, 2005).

CNTs are allotropes of carbon with a cylindrical nanostructure which are also known as tubular fullerences or bucky tubes. CNTs naturally align themselves into "ropes" held together by Van der Waals forces.

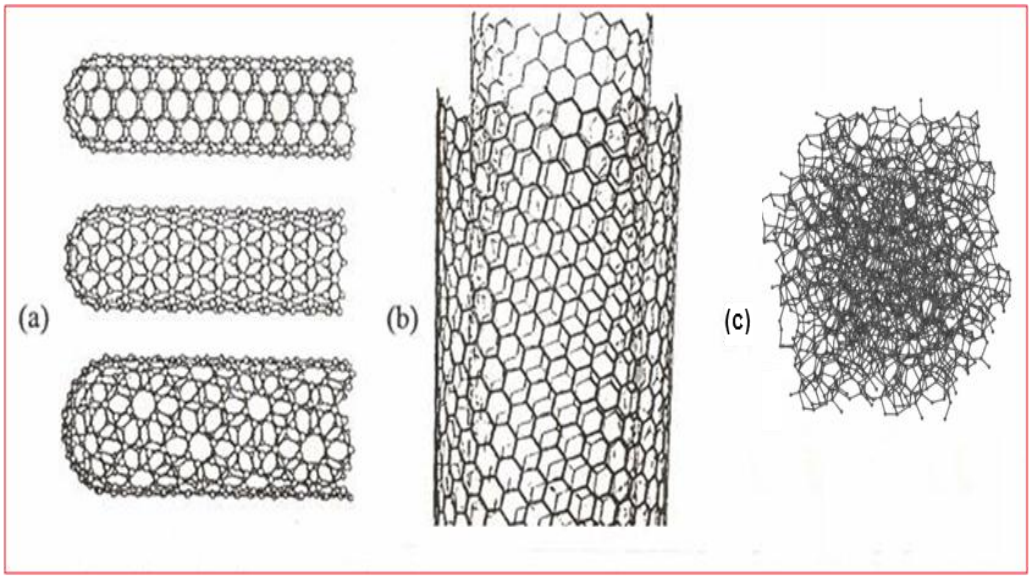

Figure 2.1: Types of carbon nanotubes of (a) SWCNTs; (b) MWCNTs and (c) α-CNTs (Peter, 2009).

CNTs can be multi-walled with a central tubule in nanometric diameter surrounded by certain amount of graphitic layers separated by about few angstroms, which are called as multi-walled carbon nanotubes (MWCNTs). Unlike MWCNTs,

single-walled nanotubes (SWCNTs) are composed of only one tubule with no other surrounding graphitic layers. Meanwhile, double-walled carbon nanotubes (DWCNTs) are similar as SWCNTs. Different types of CNTs are shown in Figure 2.1. The structure of DWCNTs is made of a tubule encircled by one graphitic layer. Interestingly, MWCNTs, DWCNTs and SWCNTs possess a same feature. They are crystalline nanotubes that have long-range periodicity in their structures and results in a definite helicity or chirality as their primitive lattice vector can be defined (O'Connell, 2006).

As mentioned before, all crystalline CNTs can be represented by a pair of indices (*n*, *m*) called the chiral vector, which relates the amount of rotation that a tube has, and is closely related to the tube's physical properties, like diameter and electronic character. Unlike the one dimensional crystalline CNTs such as MWCNTs, SWCNTs and DWCNTs, another common type known as amorphous CNTs (α-CNTs) do not have a certain long-range periodicity in their structures, thus have no definite helicity. It is because α-CNTs have high disordered structures with the presence of defects (Rakitin *et al*, 2000; Jha *et al*, 2011). In general, α-CNT consists of amorphous carbon that is a disordered, three-dimensional material in which sp^2 and sp^3 hybridization are both present in random manner (Saito *et al*, 1998). In contrast, according to another work, the walls of α-CNTs are said to compose of many carbon clusters whose characteristic is of short-distance order and long-distance order. Therefore, the properties of crystalline CNTs are different from α-CNTs (Zhao *et al*, 2006).

Nanomaterials that currently being fabricated into nanotubes from various materials such as boron nitride, molybdenum, carbon and others are one of the promising groups of nanostructured materials. However, at the moment, CNTs seem to be superior and most important due to their unique structure with interesting properties (Meyyappan, 2005).

CNTs have length-to-diameter ratio of up to 132,000,000:1, which is significantly larger than any other material (Wang *et al,* 2009).They exhibit extraordinary strength, unique electrical properties, and efficient thermal conductivity which suit them to a tremendously diverse range of applications. The breadth of applications for CNTs is indeed wide ranging: micro or nanoscale electronics, quantum wire interconnects, field emission devices, composites, chemical sensors, biomedical devices, nanocomposites, gas storage media, scanning probe tips, etc (Meyyappan, 2005; Peter, 2009).

A previous work indicates that α-CNTs have good electronic conductivity. There is no need of chirality separation for metallic or semiconductive nanotube compared to the crystalline CNTs with different band structures. Thus, α-CNTs are favourable for certain applications such as in some nanoelectronics and sensor devices (Chik *et al*, 2004).

Furthermore, these amorphous nanotubes are capable of showing impressive field emission properties in some previous works (Ahmed *et al*, 2007a; Ahmed *et al*, 2007b). Any possible problem due to chirality is absence for α-CNTs (Rakitin *et al*, 2000).

However, α-CNTs were easily self-agglomerated and bound together due to their high van der Waals force, surface area, and high aspect ratio. Additional processes such as oxidation and functionalization are necessary to modify chemically the surface of nanotubes and thus reduce agglomeration (Gojny *et al*, 2003). Besides, some properties of nanotubes could be enhanced. The field emission property of the stearic acid functionalized α-CNTs had been improved (Jha *et al*, 2011).

The mechanical characteristic of α-CNTs depend on the strength of its interatomic bonds. The nanotubes are flexible, can be elongated, twisted, flattened, or bent into circles before fracturing due to their 'twist-like' nanostructures (Saito *et al*, 1998; Melissa *et al*, 2007; Peter,2009). They may have similar thermal properties at room and elevated temperatures but unusual behaviour at low temperature because of the effect of phonon quantization (Meyappan, 2005).

2.4 Synthesis Techniques of Producing CNTs

There are many methods that have been developed for producing crystalline and amorphous CNTs. In this section, we briefly outline several popular methods used in producing CNTs.

2.4.1 Methods for producing Crystalline CNTs

Methods developed so far in synthesizing crystalline CNTs including chemical vapor deposition (CVD), electric arc discharge, laser vaporization, laser ablation, pyrolysis, high temperature hydrothermal and low- and high-temperature solvothermal but the three main methods are the CVD, electric arc discharge, and laser ablation.

2.4.1.1 Chemical Vapour Deposition (CVD)

Vapour deposition may be defined as the condensation of elements or compounds from the vapour state to form solid deposits. In chemical vapour deposition, where deposits are formed by chemical reactions which take place on, at, or near the deposition surface.CVD is a method of plating in which the deposits are produced by heterogeneous gas-solid or gas-liquid chemical reactions at the surface of a substrate. A volatile compound of the element or substance to be deposited is vaporized and the vapour thermally decomposed, or reacted with other gases or vapours, at the substrate as a coating. By reason of the very large number of available chemical reactions, chemical vapour deposition is seen to be a process of potentially great complexity as well as one of

great versatility and flexibility. CVD has the greatest throwing power, that is, the ability to deposit uniformly on relatively complex shapes, and it is applicable to the widest range of materials (Blocher, 1966).

The CVD method is believed as the most suitable CNT synthesis method in terms of product purity and large scale production. In this method, a substrate is prepared with a layer of metal catalyst particles, most commonly nickel, cobalt, iron, or a combination of these materials. The diameter of the grown nanotubes is related to the size of the metal particles. To initiate the growth of nanotubes, two gases are bled into the reactor: a process gas (such as ammonia, nitrogen, hydrogen, etc) and a carbon-containing gas (such as acetylene, ethylene, ethanol, methane, etc) (Ren *et al*, 1998;Singh *et al*, 2002).

It is reported that the reaction temperature plays an important role in alignment properties and diameter of the synthesized of CNTs (MacKenzie *et al*, 2009). Generally, CNT growth temperature used is between 550°C and 1000°C, and the reaction temperature may vary according to the catalyst-support material pair. Also, the variations in the optimum gas (carbon source) flow rate and inert gas flow rate result in the decrease in the CNT yield. Most widely used inert gases are argon and nitrogen with a flow rate of around 100mL/min. Sometimes, inert gas is changed with hydrogen gas to reduce the oxygen content in the reaction environment (MacKenzie *et al*, 2009). Figure 2.2 shows a schematic diagram for CNT growth by CVD method in its simplest form.

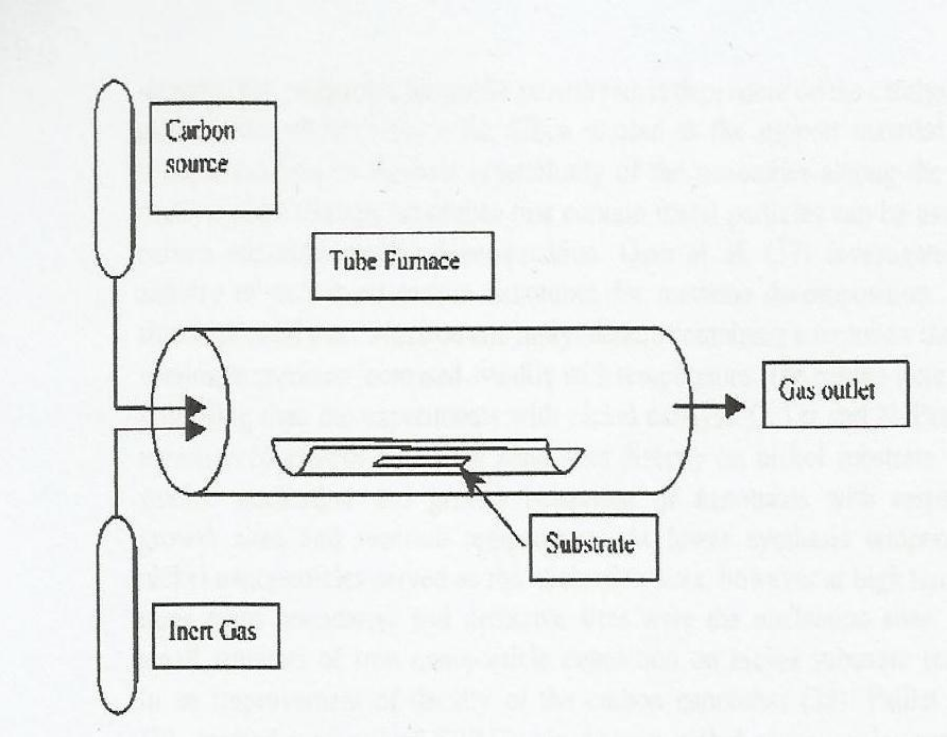

Figure 2.2: Schematic diagram of a typical thermal CVD (Oncel, 2004)

2.4.1.2 Arc Discharge

Among several methods for preparing CNTs, arc discharge is the most practical for scientific purposes because the method yields highly graphitized tubes due to the high process temperature (Keidar *et al*, 2004). However, besides CNTs, arc discharge methods produce many by-products. As a result, the process requires complicated and well controlled purification steps (Ebbesen *et al*, 1992).Figure 2.3 shows a schematic diagram of dc arc diagram.

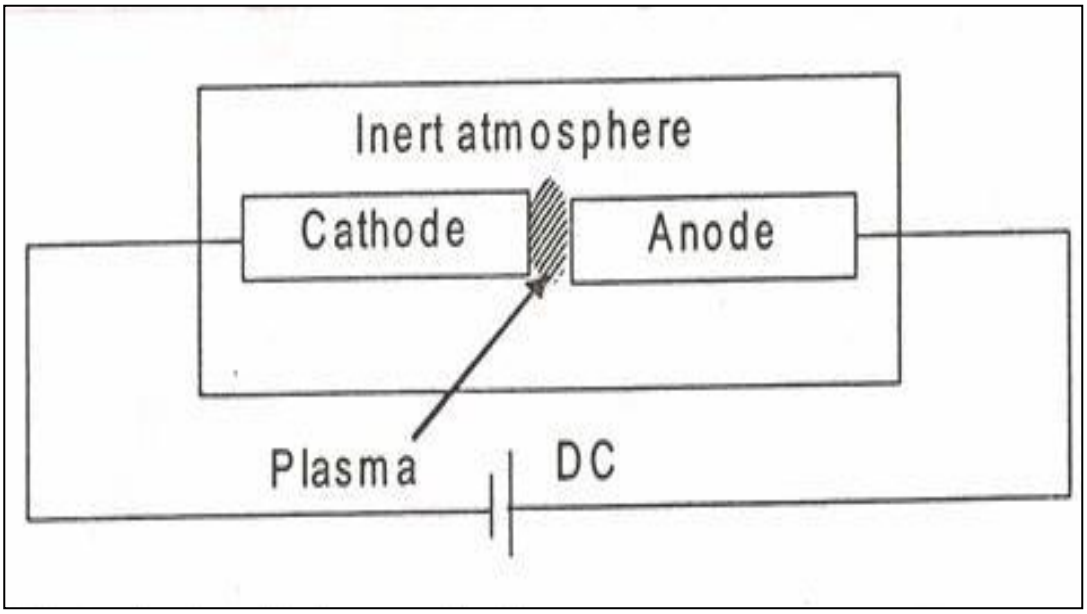

Figure 2.3: Schematic diagram of the arc discharge method (Meyyappan, 2005).

Relatively large scale yield of CNTs (≈75 %) was produced at 100 - 500 Torr He and about 18 VDC (Ebbesen *et al*, 1992). Typical nanotubes deposition rate was around 1 mm/min. The incorporation of transition metals such as Co, Ni or Fe into the electrodes as catalyst favors crystalline CNTs formation against other nanoparticles and reduced operating temperature. However, the arc discharge unit must require cooling system whether catalyst is used or not. This is to prevent overheating that will result safety hazards and coalescence of the nanotube structure. CNTs with smaller diameter between 2 - 30 nm and length 1 µm can be deposited on the cathode via this method as revealed by transmission electron microscope (TEM) analysis (Peter, 2009).

MWCNTs were first discovered on the cathode surface by Ijima (Iijima, 1991). Sooner, larger amount of MWCNTs in gram with diameter of about 14 nm had been found successfully (Ebbesen *et al,* 1992).

The choice of metal catalyst for this process determines primarily the yields of SWCNTs. The combination of two different types of metal had produced much higher yields of SWCNTs than did individual metals (Serapin *et al,* 1994). The synthesis of DWCNTs was a challenge for a long time. The breakthrough of DWCNTs was made with the arc discharge technique (Hutchison *et al,* 2001). Most DWCNTs had an outer diameter in range 3 - 5 nm with wall separation distance of 0.39 ± 0.02 nm. Larger diameter generally corresponds to higher process temperature.

2.4.1.3 Laser Ablation

In laser ablation, carbon nanotubes form in the plume of carbon vapour evaporated by a laser from a graphite target held at 1200°C. The nanotubes develop on the cooler surface of the reactor, as the vaporized carbon condenses. The yield of nanotube synthesis by this process is about 70%. The nanotubes generated by the above mentioned methods are relatively impure, with presence of unwanted carbonaceous impurities. The resulting products are swept from the high temperature zone by using an inert gas and conical copper head is used to deposit the nanotubes. These methods are also not operated at higher scale, therefore, and the overall production costs are high (Mittal, 2010).

2.4.1.4 Hydrothermal Synthesis

Carbon nanotubes tend to be in a state of an entangled mass because of their flexible fiber-like structure and also the consequence of the strong attractive forces between them. This makes the dispersion process a compelling crucial factor in obtaining functional CNT-reinforced composites. Before mixing of CNTs and ceramic powders, carbon nanotubes have to be functionalized for the homogeneous dispersion. The generally implemented method includes the acid treatment which induces defects on the nanotubes (Yamamoto *et al,* 2008). Therefore acid treated CNTs possess limited strength and conductivity. But, hydrothermal synthesis can provide an environment for nanotubes to be functionalized while giving little or no harm, unlike acid treatment (Zaman *et al*, 2010) becausethe high temperatures and pressures may break the hard big agglomerates of CNTs and force functional groups (COOH, OH) to attach on the sidewalls and open ends of CNTs under thepresence of appropriate chemicals, repulsion between individual tubes can be maintained during hydrothermal synthesis (Zaman *et al*, 2010). Hydrothermal processing can be defined as any heterogeneous chemical reaction in the presence of a solvent (whether aqueous or non-aqueous) under high pressure and temperature conditions at pressure greater than 1 atm in a closed system (Byrappa and Adschiri, 2007).

Deposition and patterning of layers of Ni as a catalytic material can easily be accomplished by the hydrothermal technique (or electrodeposition) on a variety of substrates, even at room temperature , which indicates that hydrothermal processing could be applied in this case for the entire device fabrication (Yoshimura *et al*, 2000).

The hydrothermal technique is known to give products with a much higher homogeneity than solid state processing and with higher density than gas or vacuum processing (faster growth rate). Moreover, liquids accelerate diffusion, adsorption, reaction rate, and crystallization (nucleation and growth), especially under hydrothermal conditions (Yoshimura and Suchanek, 1997). Under supercritical conditions, the fluid has some of the advantages of both a liquid and a gas. Diffusion in supercritical fluids is higher than that in liquids and the viscosity is lower, enhancing the mass transport (Eckert *et al*, 1996). These phenomena usually contribute to a significantly increased yield of synthesized materials, as compared to deposition from the gas phase (Yoshimura *et al*, 2000).

2.4.2 Methods for producing Amorphous CNTs

In this section, we briefly outline the methods used for producing α-CNTs.

2.4.2.1 Chemical Vapor Deposition (CVD)

In a previous work, by using suitable catalyst, like Ni-Al or nickel particles supported on alumina catalyst, carbon source such as methane (60ml/min) and hydrogen (420ml/min) as the carrier gas, the CVD process was carried out at 480 °C for 30 min followed by a cooling process to room temperature under an nitrogen atmosphere (Zhao, 2006; Yacaman *et al*, 1993).The successfully produced α-CNTs from this needed catalyst method was mostly governed by the cooperative function of a low temperature and hydrogen carrier gas.

2.4.2.2 Arc Discharge

There are also studies on producing α-CNTs using arc discharge. Electric arc discharge is the classic technique in which an arc is created between a graphite cathode and a graphite anode. By adding a catalyst such as Co, Ni and Fe, CNTs condense on the surface of the cathode.

Amorphous CNTs (α-CNTs) can also be produced by using DC arc discharge. Typically, an arc discharge was carried out in an atmosphere of hydrogen gas at a pressure of 50 kPa. The arc current was maintained at 80-100A. An inner stainless steel chamber containing raw materials and Co-Ni alloy powders as catalyst was mounted on a DC arc discharge furnace with a temperature controlling system. The temperature was controlled by a thermocouple during heating and arc discharge. After a certain time of evaporation, the soot (α-CNTs) with small crystalline component was observed on the wall of the inner chamber and also around the anode and cathode rods. Typically, α-CNTs with diameter in range 10 - 15 nm had been synthesized with the presence of ferrous sulfide (FeS) served as catalyst (Liu YN *et al*, 2004).

There was a modified arc discharge being conducted and had successfully produced α-CNTs with diameter about 7 - 20 nm (Nishino *et al*, 2003). It was found that the cooling rates and types of the gas, the temperature in the furnace and the catalyst all play an important role in this process. The furnace temperature has a large effect on the α-CNT diameter because the diameter increases with increasing temperature. The growth mechanism was explained that the random deposition of small carbon clusters from the

gas phase on to a straight template of iron halide. Due to fast cooling rate of hydrogen gas, the carbon clusters are easily formed before atoms deposit onto the catalyst to form a crystal structure. Instead of forming long distance ordered crystalline tubes due to the lack of enough energy and time, the clusters formed the disordered structures which called as amorphous nanotubes (Tingkai, 2005).

2.4.2.3 Template-Confined Growth

Template-confined growth has advantages by obtaining aligned nanomaterials with adjustable diameter, length and morphology. Actually, mesoporous silica template was the first template to form aligned CNTs (Li *et al*, 1996).

Due to the different channel structures of the porous anodic aluminum oxide AAO which is a widely used template, the morphology of the CNTs inside the channels could be conveniently regulated by altering anodization parameters (Wang *et al*, 2002).

Normally the wall structures for CNTs grown within AAO template are highly disordered and are different from those synthesized by arc discharge or laser ablation (Sui *et al*, 2001). The highly disordered α-CNTs formed within AAO templates could probably possess uniform properties due to the homogeneity, by analogy with the case for amorphous alloys (Yang *et al*, 2003).

In the year of 2003, α-CNTs with amorphous structure and irregular end had been successfully prepared by AAO template-confined through the pyrolysis of acetylene with the presence of Ni catalyst. The formation of disordered structure of nanotubes was as the result of the lattice mismatch between alumina and carbon species. The aligned arrays, Y-branched as well as novel dendriform nanotubes had been revealed (Yang *et al*, 2003). In the recent year, another work that used similar approach to produce α-CNTs by a relatively simple template at low temperature of 450°C. The absence of catalyst resulted in the final product free of any contaminations and purification steps (Zhao *et al*, 2009). AAO was used as template and citric acid was acted as precursor. AAO template was prepared by a conventional two-step anodic process (Wang *et al*, 2002).

This work was claimed that the diameter, length and even the wall thickness of the walls of α-CNTs could be tuned by changing the pore diameter and the thickness of AAO templates, respectively. Besides, the orientation of graphene layers and the graphitization degree could be controlled by the pH of the citric acid solution.

1.5 Hybrid Carbon Nanotubes

Copper oxides are semiconductors and have been studied for applications including rectifying and microwave diodes and solar cells. The use of copper oxide in solar cells has been extensively reported (Zhu *et al*, 2008). Cuprous oxide (Cu_2O) is a p-type semiconductor having a band gap of 2.0 eV and monoclinic crystal structure (Balamurunga, 2001). Apart from their semiconductor applications, these materials have been employed as heterogenous catalysts for several environmental processes, solidstate gas sensor heterocontacts and microwave dielectric materials (Morales *et al*, 2005). Besides, copper oxides have been used as electrode materials for lithium batteries (Souza *et al*, 2004; Souza *et al*, 2006).

These materials have unique features such as their low cost, non-toxicity, the abundant availability of copper, a theoretical solar cell efficiency of 18% and relatively simple formation of the oxide layer (Ghosh *et al*, 2000). Therefore, copper oxides become a focus of this work to hybrid with α-CNTs. However, preparation of these hybridized materials has not been clearly understood and reported. This work is to explore the properties of this hybridization material. Cu_2O is the most studied because of its high optical absorption coefficient in the visible range and shows good electrical properties (Rakshani, 1986).

CHAPTER THREE

METHODOLOGY

1.1 Raw Materials

The main precursor materials used in this work were ferrocene ($Fe(C_5H_5)_2$) and ammonium chloride (NH_4Cl) powders. $Fe(C_5H_5)_2$ powder with purity of 98 % was produced by ACROS Organics. It is an organometallic compound a type of organometallic chemical compound which consisting of two cyclopentadienyl rings bound on opposite sides of a central metal atom. It acted as carbon source for the formation of α-CNTs. On the other hand, NH_4Cl compound with analytical grade was used as catalyst during the reaction.

For purification treatment, diluted hydrochloric acid (HCl) in molarity of 5 M, and deionized water were used. The purified α-CNTs were then hybridized by copper oxide. The usage of $Fe(C_5H_5)_2$, the preparation of acid solutions into suitable concentration had been conducted under a fume hood due to the strong characteristic odour and safety purpose. All mentioned analytical chemicals were used as received without any further purification. The experiment has been carried out at Advanced Material Lab.

3.2 Preparation of Amorphous Carbon Nanotubes

This study involves three main processes which are heating, purification and hybrid process to synthesis Cu_2O-CNT hybrid. The schematic of the sequences of the research work are shown in Figure 3.1.

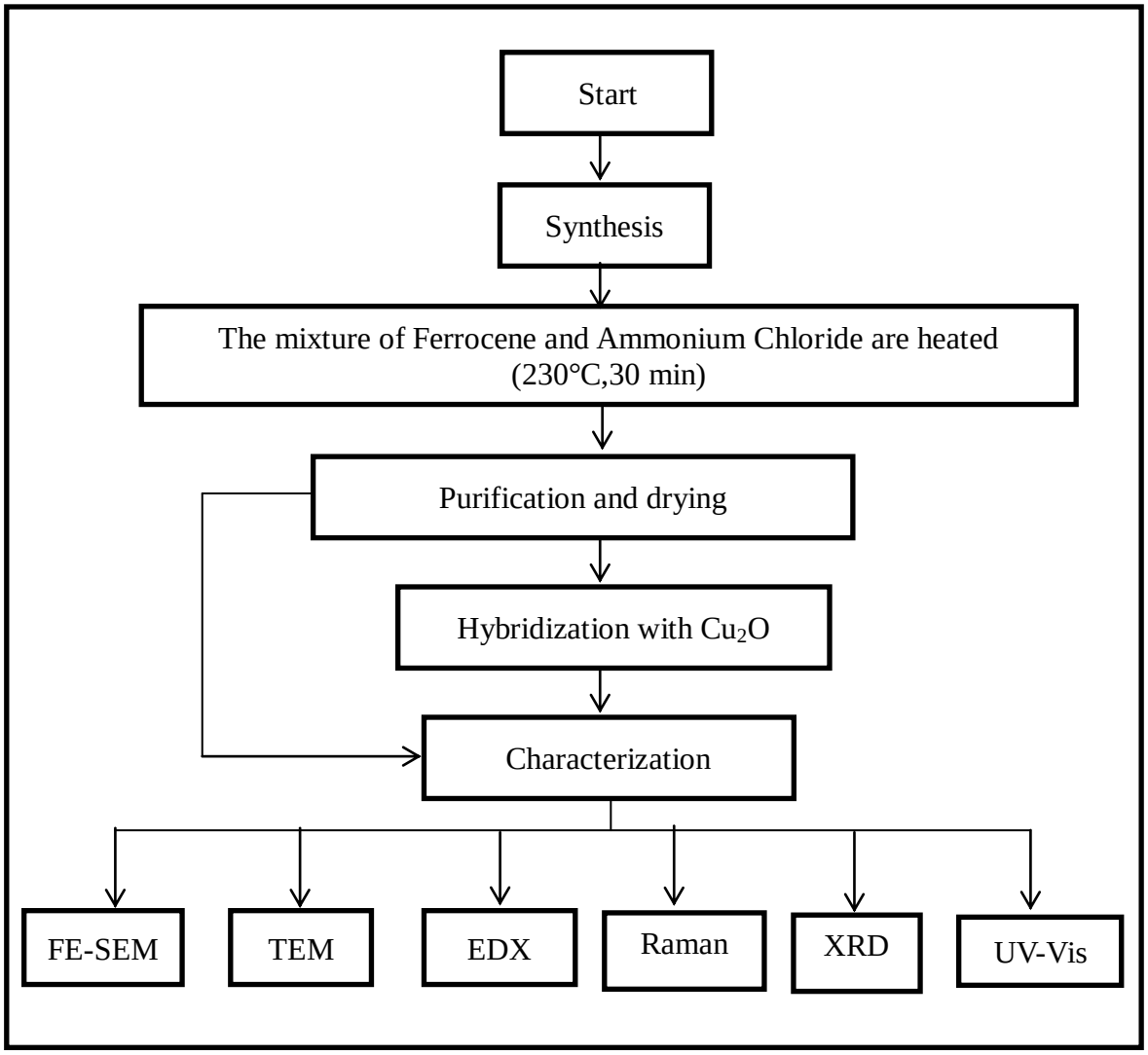

Figure 3.1: Flow chart of the work.

In this work, all as-prepared samples, α-CNTs were synthesized via a modified reduction process. A mixture of both powdered NH_4Cl (analytical grade) and $Fe(C_5H_5)_2$ (ALDRICH Chemistry, 98 %) was placed in a clay crucible (4 and 2 g, respectively) to be heated in a convection furnace.For the purpose of heating the mixture to high temperature, the mixture was then heated in a clay crucible which can withstand high temperature, with the capacity of 50 mL. The clay crucible was covered and heated to 230 °C inside a furnace. The mixture was hold at this temperature for 30 minutes. After the crucible was cooled down to room temperature, the mixture was taken out and again being mixed homogeneously. The whole heating process was repeated again for 30 minutes. The obtained black powder was named as untreated sample (as-prepared sample).

Purification of the as-prepared sample is necessary. In order to get rid of any other impurities via purification, the untreated sample was soaked and washed with hydrochloric acid, HCl in 5 M, followed by distilled water. These processes were carried out for several times for better purification efficiency. Filtrate was collected on nylon filter membrane (0.2 μm) with aid of a pump. Dehydration was performed to obtain the final sample, which was named as treated sample by using a vacuum oven at 80 °C for 10 h.

The washed sample was then hybridized by copper dioxide via a simple route. The copper dioxide was dissolved in ethanol solution of 10 ml and ultrasonicated for 2 hours.

On the other hand, the treated sample was dissolved in ethanol solution of 40 ml and ultrasonicated for 20 min. Both dissolved solution were then mixed together with certain combination of compositions as shown in Table 3.1.The mixture was stirred for 20 h to facilitate hybridization between amorphous nanotubes and copper dioxide and finally was ultrasonicated for 2 hours which can help to break up agglomerated nanotubes.

Table 3.1 Weight compositions of Cu_2O and CNT

Samples	**Cu_2O mass (g)**	**Treated CNT mass (g)**
A	0.2	0.1
B	0.4	0.1
C	0.6	0.1
D	0.8	0.1
E	1.0	0.1

3.3 Characterization Methods

All the samples (untreated sample, treated sample, andhybridized sample) were studied by few characterization methods which could be divided into four aspects: morphological studies, microstructural studies, elemental analysis and optical studies.

3.3.1. Morphological Studies

Samples were observed under TEM (LIBRA® 120, Germany) and FE-SEM (AURIGA, ZEISS, Germany) to perform a qualitative analysis on the nanotubes surface morphology and microstructure. The used TEM was operated using an accelerating voltage of 120 kV. The FE-SEM was equipped with detectors of secondary electrons and an EDX spectrometer. The micrographs were generated by backscattered electron detector in FE-SEM. All of these characterization methods could estimate the morphology and geometry (diameter) of nanotubes.

3.3.2. Microstructural Studies

Microstructural analysis was studied by using XRD (SIEMENS D5000, German) with Cu-K α X-radiation of wavelength 1.54056 Å at 60kV and 60 mA. The diffraction was conducted in the Bragg angles between 5 ° to 100° in order to examine the crystallinity of nanotubes and Cu_2O. The presence of elements could also be performed and identified.

3.3.3. Elemental Studies

EDX spectrometer embedded in FE-SEM equipments was employed to conduct elemental analysis on the nanotubes at room temperature. During an observation, EDX test was performed under the STEM mode. The EDX test was also carried out by the FE-SEM. The EDX was conducted after HRTEM and FE-SEM images being captured. The voltage used for this test should be more than 10 kV and located at 8 mm working distance in order to obtain better quantitative elemental analysis.

3.3.4. Optical Studies

The UV-Vis optical absorption was recorded using a spectrophotometry (Cary Win UV 50, Australia). By using a 1 cm quartz cuvette, the optical absorption and transmittance measurement were then scanned at slow rate over the range 200 - 800 nm (ultraviolet, infrared, visible and adjacent regions). Prior to UV-Vis measurement, ultrasonication process was performed towards a sample containing nanotubes in ethanol as solvent for 2 hours in order to provide better dispersion of the sample.

The optical band gap (E_g) for the α-CNTs is estimated by using Tauc/Davis-Mott model based on the measurement of optical absorption as this value are important parameter for the optoelectronic applications (Li *et al.*, 2009). According to the mentioned model, the relation between E_g and optical absorption is expressed by Eq. (1):

$$(\alpha h\nu)^n = \mathrm{B}\,(h\nu - E_g) \qquad (1)$$

where B is a constant, $h\nu$ is the photon energy of the incident light and n is the characterization index for the type of optical transition. The absorption coefficient (α) is defined by the Lambert-Beer law as Eq. (2):

$$\alpha = - \ln A / t \quad (2)$$

where A is absorbance and t is the sample thickness. The optical band gap can be obtained from the extrapolation of the best linear parts of the curves for $(\alpha h\nu)^n$ versus $h\nu$ at α is zero near the band edge region.

Raman spectroscopy which acted as a method for detection of nanotubes in nanotubes in bulk samples were also performed to provide deep and comprehensive understanding on the structure of the nanotubes. Raman characteristics of the α-CNTs were conducted with wavelength in the range from 200 nm to 800 nm.The measurements were taken for all samples.

CHAPTER FOUR

RESULTS AND DISCUSSION

This chapter presents the results of the synthesis and characterization of α-CNT and α-CNT hybrid with Cu_2O. Synthesis studies were carried out in order to understand the properties of new materials.

Morphological Studies

4.1.1 Field Emission Scanning Electron Microscopy (FE-SEM) Analysis.

Field Emission Electron Microscopy (FE-SEM) images of all the α-CNTs samples are shown in Figures 4.1-4.3. Figure 4.1 (a) shows a low magnification image of untreated α-CNTs. From the figure it is clear that the tubular structure is formed and the nanotubes are closely attached to each other. Figure 4.1 (b) shows the higher magnification image of untreated α-CNTs where it can be clearly seen that many α-CNTs are closely bound together. The open end of the tubes can be clearly seen in this figure. Also from this figure, the tubular structure of the α-CNTs are clearly visible with inner diameter 45 nm while the outer diameters are 100 nm.

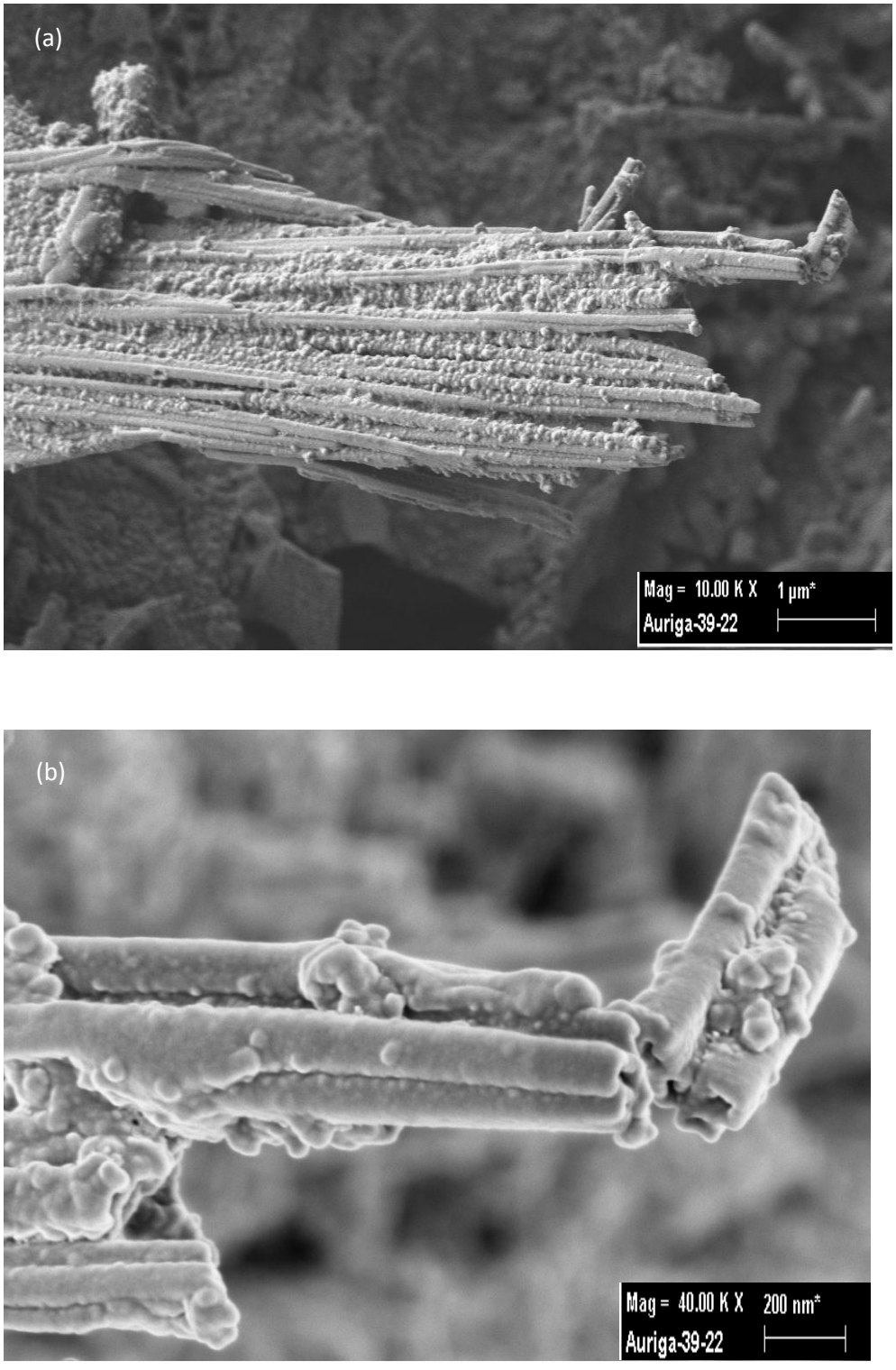

Figure 4.1: FE-SEM images of the untreated α-CNTs with different magnifications:

(a) 10,000X (b) 40,000X

Figure 4.2 (a - b) show the FE-SEM images of the α-CNTs after purification process through HCl and deionized water. It can be seen from Figure 4.2 (a) that the nanotubes, which were compactly bound previously, are now tending to separate from each other due to acid treatment. This indicates that the agglomeration has been reduced. It can also be noticed from Figure 4.2 (a) that the surface of the nanotubes are much smooth unlike for the untreated α-CNTs.

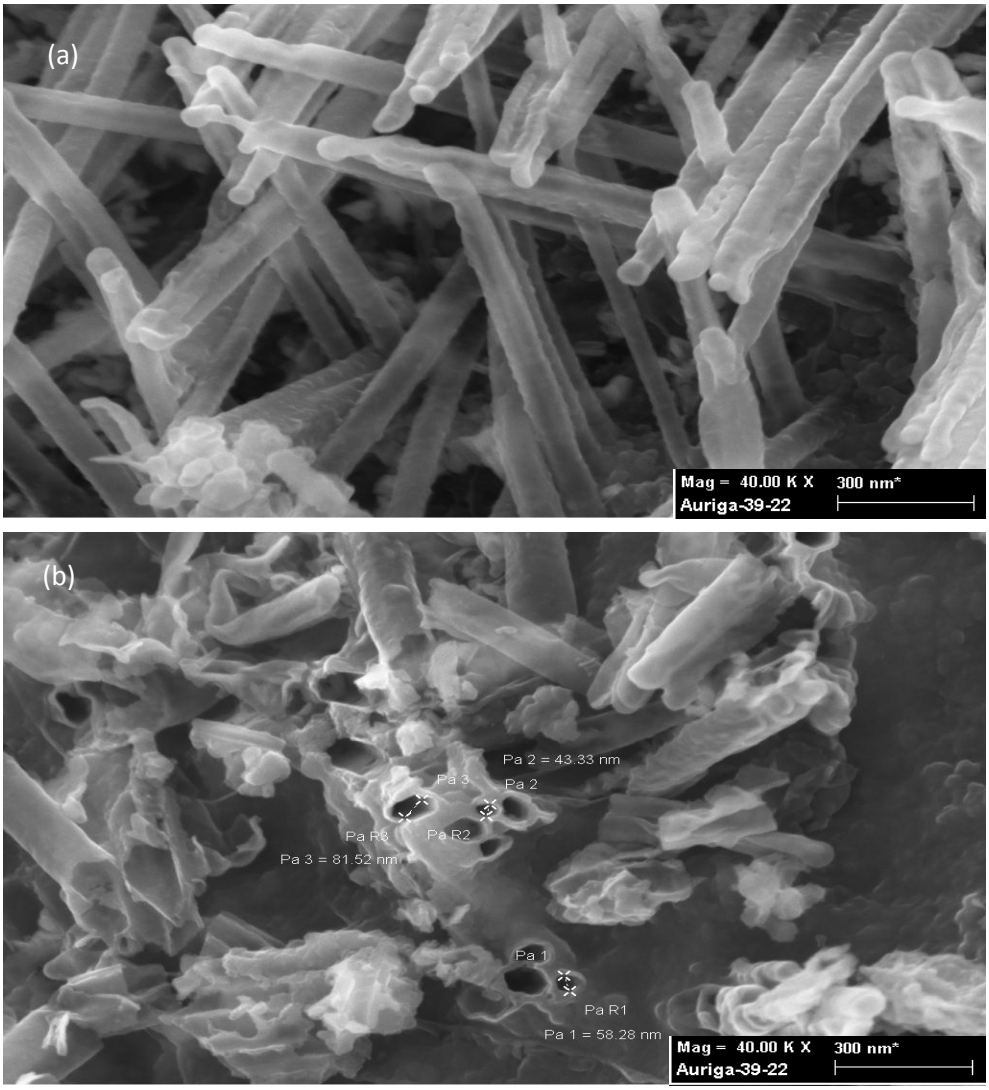

Figure 4.2 : FE-SEM images of the treated α-CNTs at same magnification.

Meanwhile, figure 4.2 (b) shows that the open ended structure of the treated α-CNTs are clearly visible with inner diameter 43 nm – 58 nm while the outer diameters are 90 nm – 150 nm.

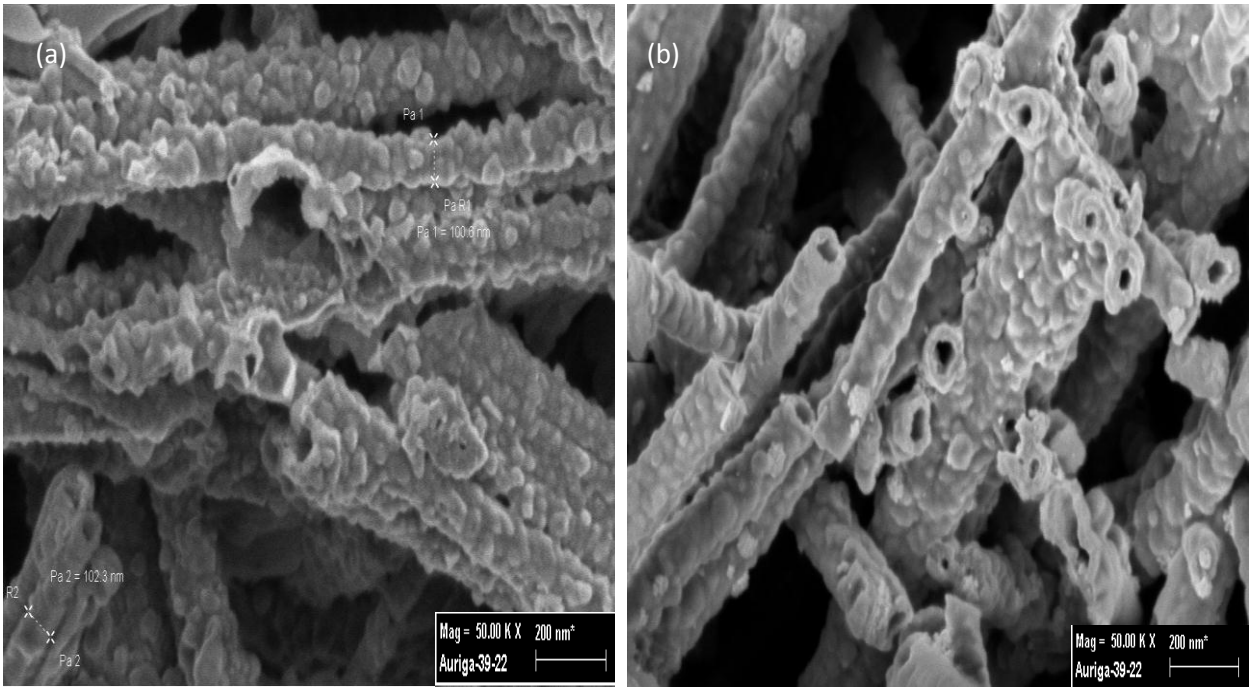

Figure 4.3 FE-SEM images of the hybridized α-CNTs-Cu_2O sample at different weight of Cu_2O: (a) 0.2 g ; (b) 1.0 g

Figure 4.3 (a - b) show the FE-SEM images of the hybrid α-CNTs-Cu_2O . It is obvious that the nanotubes are no more tightly bounded to each other and their agglomeration is highly decreased. The surface of the nanotubes are very much rough compared to non-hybrid sample. These surfaces are coated with Cu_2O indicating that the hybridization between Cu_2O and α-CNTs is possible. The outer diameters of α-CNTs-Cu_2O are measured to be around 100 nm.

4.1.2 Transmission Electron Microscopy (TEM) Analysis

Figures 4.4 -4.6 show the TEM images of α-CNTs and hybrid α-CNTs-Cu_2O.

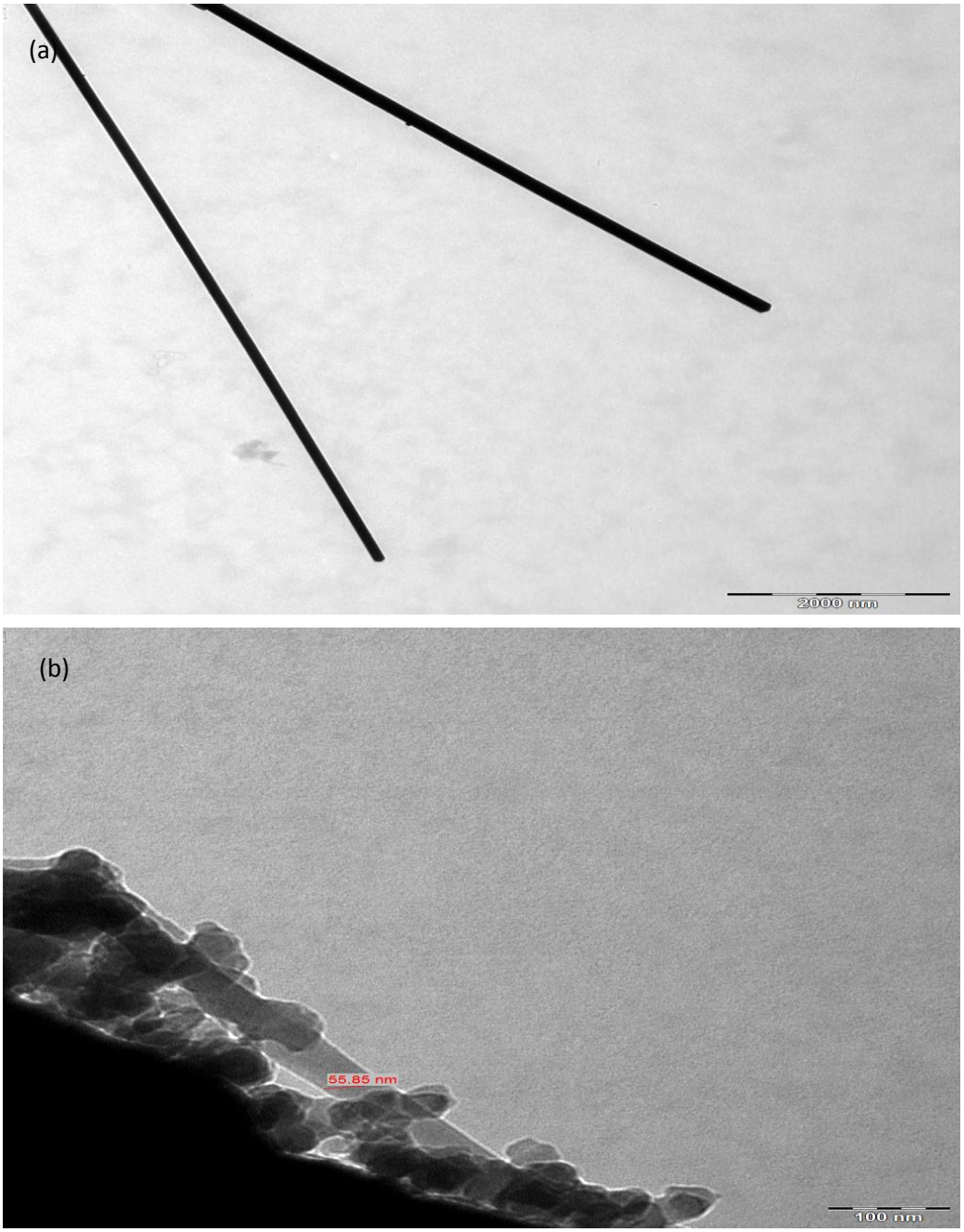

Figure 4.4 TEM images of the treated α-CNTs at different magnifications: (a) Low magnification; (b) High magnification.

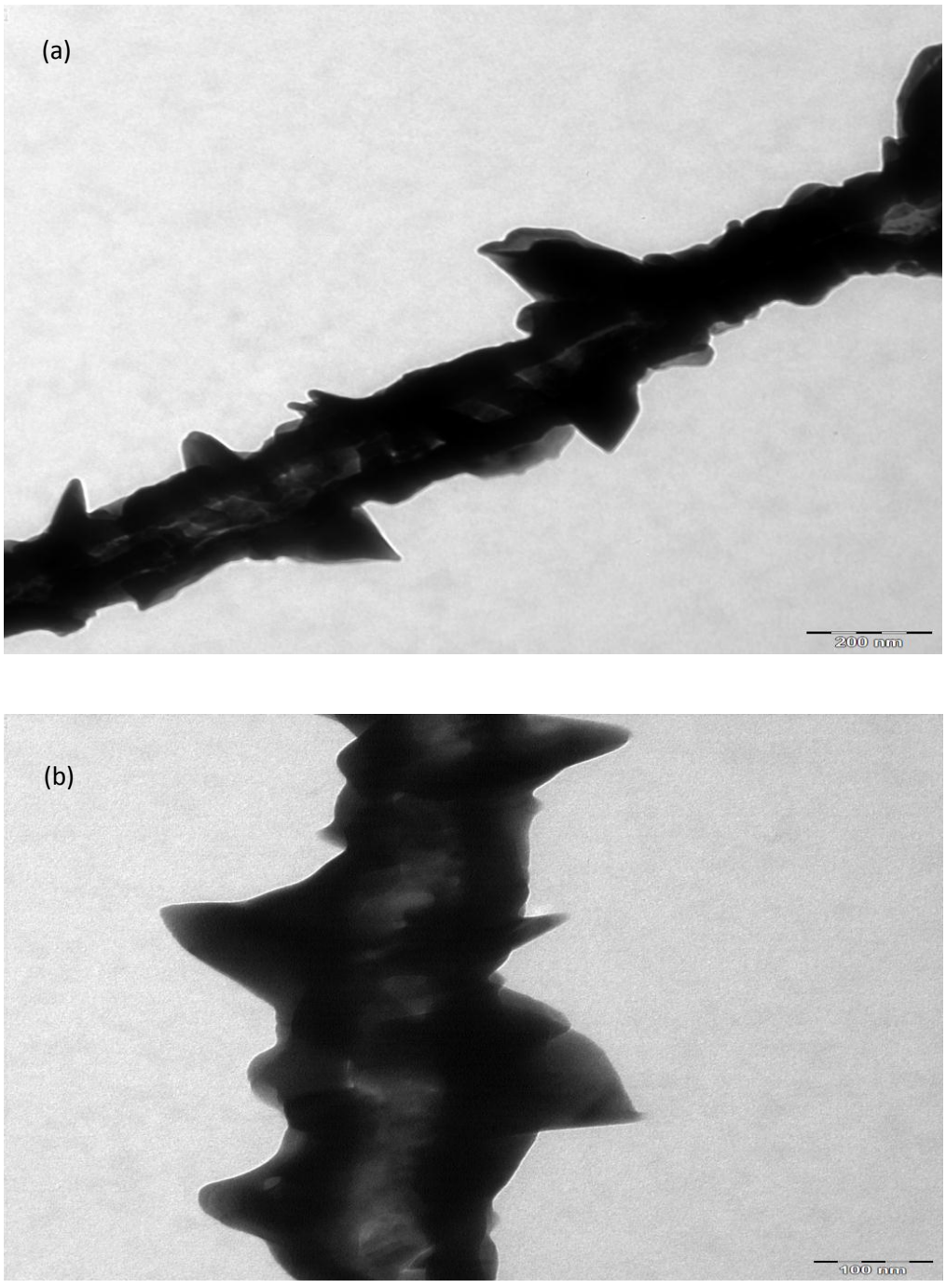

Figure 4.5: TEM images of the hybridized with 0.2 g Cu_2O at different magnifications: (a) Low magnification; (b) High magnification.

The diameters of treated α-CNTs (Figure 4.4) lie in the range of 50-100 nm. This result is comparable with the previous FE-SEM results. Figure 4.5 shows the TEM image of hybrid α-CNTs-Cu_2O. The surfaces of these nanotubes are not smooth due to the adsorption of Cu_2O on the surface of α-CNTs. The diameter of hybridized sample lie in the range of 130 - 170 nm. The increment of the diameter and the attachment at the surfaces of nanotubes confirmed that the α-CNTs were successfully hybridized by Cu_2O.

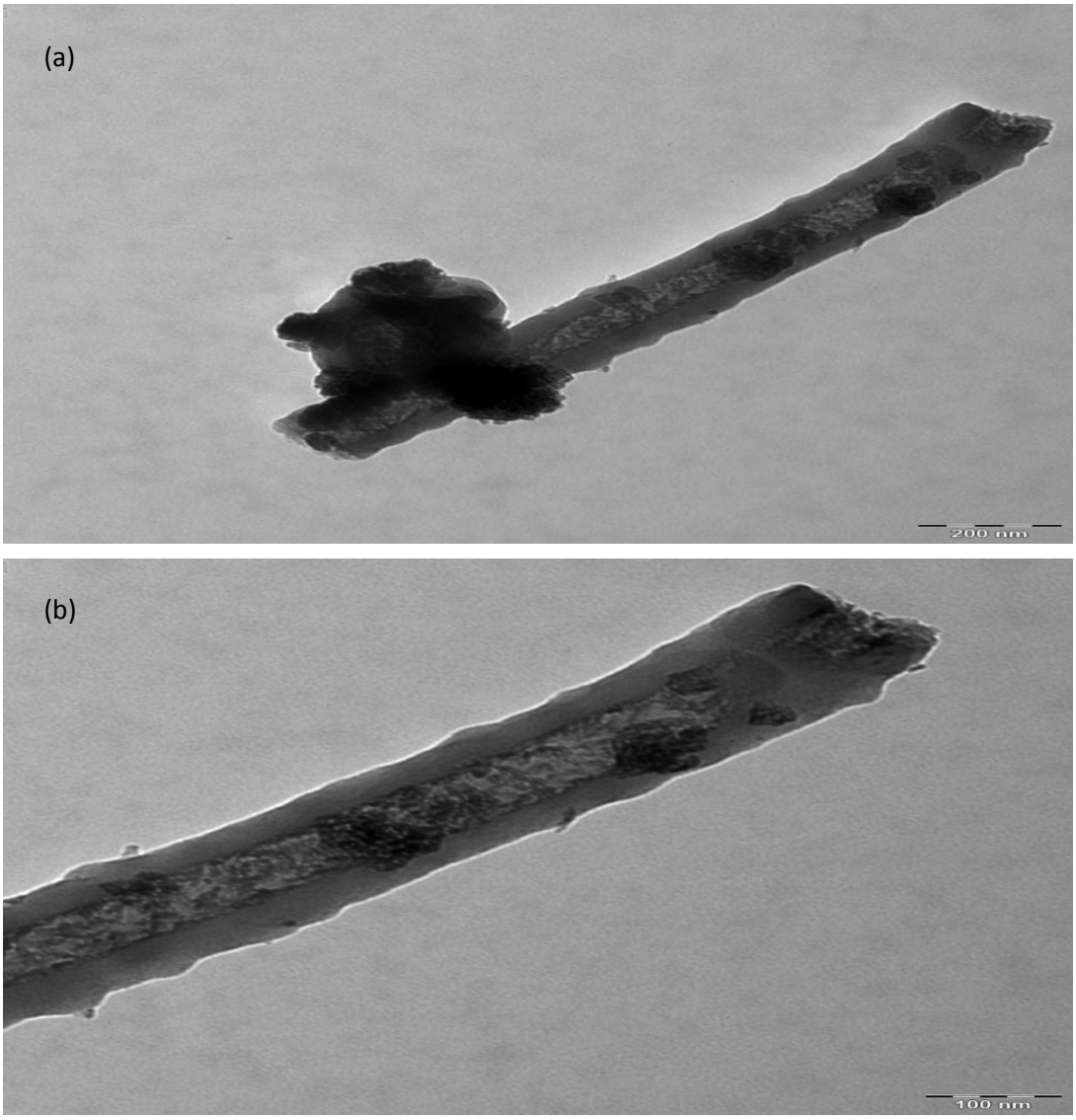

Figure 4.6: TEM images of the hybridized sample with 1.0 g Cu_2O at different magnifications: (a) Low magnification; (b) High magnification.

4.2 Microstructural Studies

4.2.1 X-ray Diffraction (XRD) analysis

Fig 4.7 shows the X-ray Diffraction patterns of all samples.

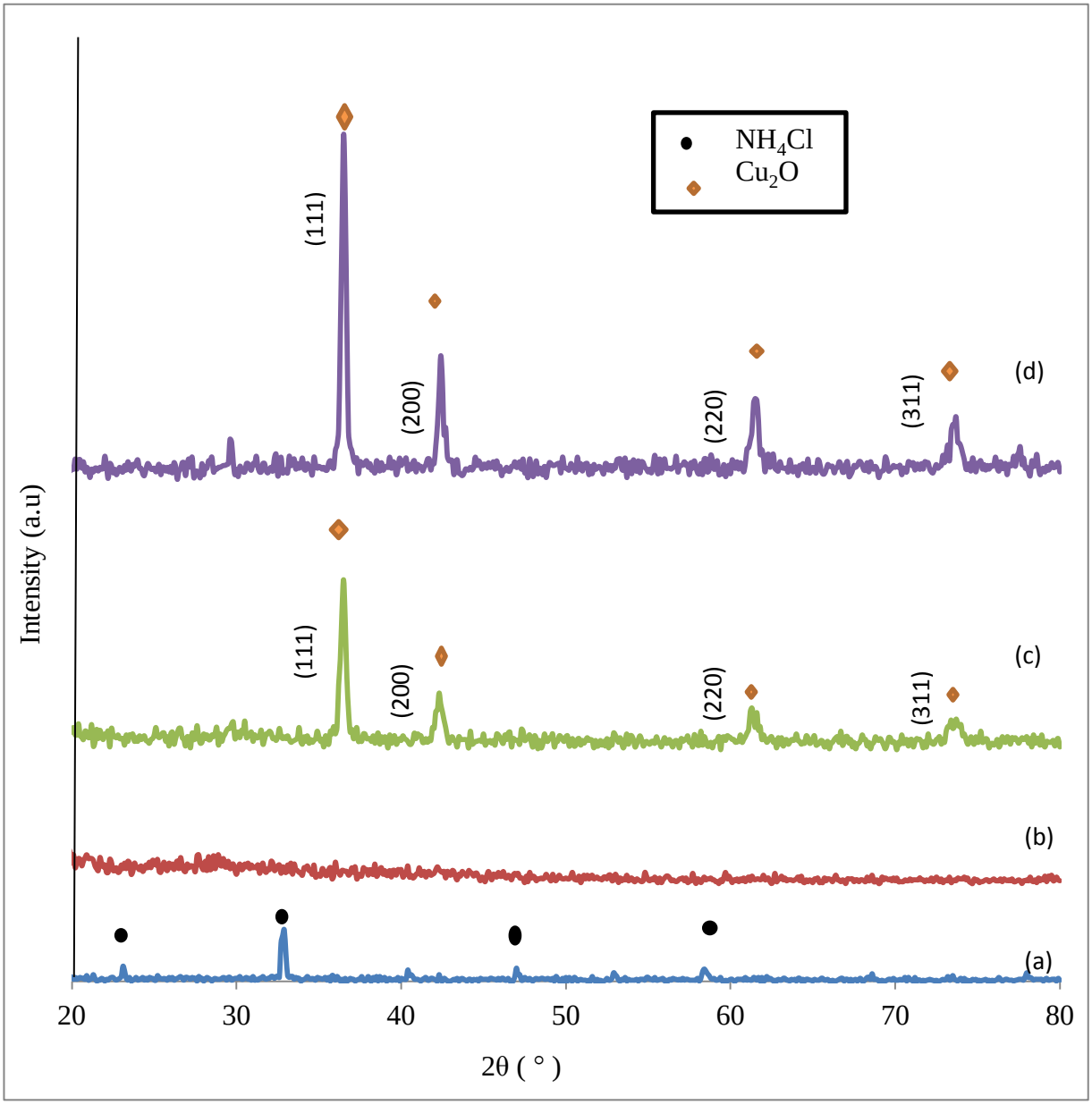

Fig 4.7 XRD pattern for: (a) Untreated α-CNTs; (b) Treated α-CNTs; (c) Hybridized sample with 0.2 g Cu_2O; (d) Hybridized sample with 1.0 g Cu_2O.

Figure 4.7 (a) shows the XRD pattern of the untreated α-CNT. Diffraction peaks were observed at angle 2θ of 22°, 32°, 41°, 46° and 58°. All these are assigned to the diffraction lines of NH_4Cl phase. These results confirm the existence of impurities in the untreated sample.

When the untreated sample was washed with HCl and deionized water for several times, pure α-CNT was obtained as shown in Figure 4.7 (b). The XRD patterns of the treated samples show no prominent peak at all, indicating a complete amorphous phase which is consistent with the results from TEM in Figure 4.5. Acid treatment does have influence on the CNTs.

Fig 4.7 (c) shows the XRD pattern of the hybrid material sample indicating several diffraction peaks at 2θ values of 36.5°, 42.5°, 61.5°and 74°. All these are (α-CNT-Cu_2O) assigned to diffraction peaks of cuprite (Cu_2O). These results confirm the formation of Cu_2O crystals on the surface of α-CNTs. It is also observed that the intensity of the peaks corresponding to higher amount of Cu_2O (Figure 4.7 d) is much stronger than that of lower amount of Cu_2O (Figure 4.7 c). This further indicates the formation of Cu_2O coated α-CNTs sample. The hybrid samples are crystalline in nature due to the adsorption of Cu_2O on the surface of α-CNTs.

4.3 Elemental Studies

4.3.1 Energy Dispersive X-ray (EDX) Analysis

Figures 4.8 (a) and (b) show the energy dispersive X-ray (EDX) spectra for untreated and treated samples.

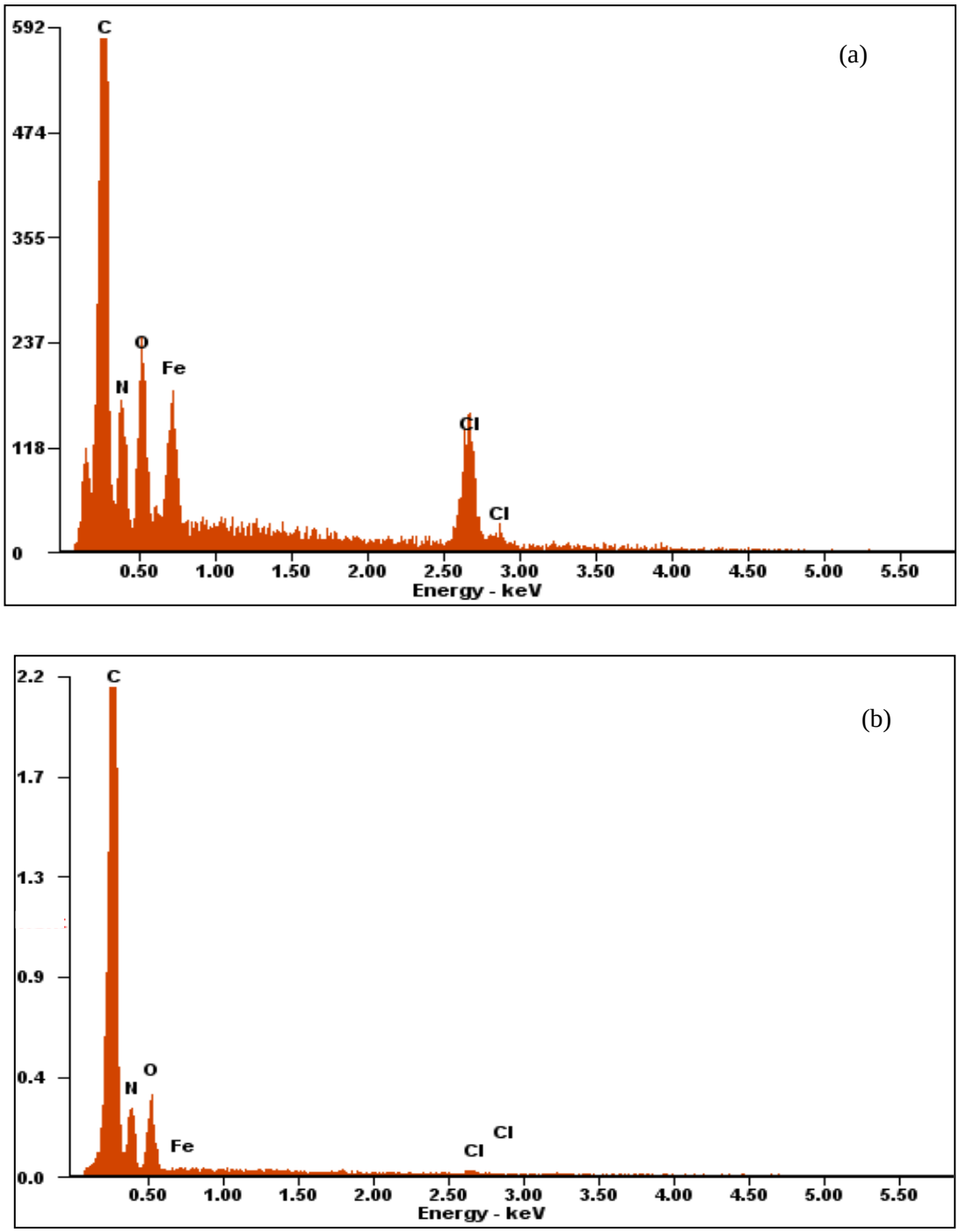

Fig. 4.8 EDX spectra of the α-CNTs for (a) Untreated α-CNTs (b) Treated α-CNTs.

The respective weight and atomic percentages for the possible elements in all of the samples are also presented in Table 4.1. The strong peak attributed to carbon is clearly present in the EDX spectra for both samples. The presence of other elements like Fe and Cl were originated from the precursors such as Ferrocene and NH_4Cl. However their amounts are greatly reduced after washing with HCl and deionized water as shown in table below.

.

Table 4.1: Elemental analysis for untreated and treated samples.

Sample		Elements				
		C	O	Cl	Fe	N
Untreated Sample	Wt%	37.44	6.14	29.65	17.92	8.86
	At%	58.92	7.25	15.81	6.06	11.96
Treated Sample	Wt%	66.65	10.44	3.35	1.43	18.15
	At%	72.85	8.56	1.24	0.34	17.01

4.4 Optical Studies

4.4.1 UV-Vis Spectroscopy Analysis

In this work, UV-Vis spectrophotometer is used to investigate the dispersion stability of nanotubes in a certain volume of alcohol (ethanol) and their optical characteristics.

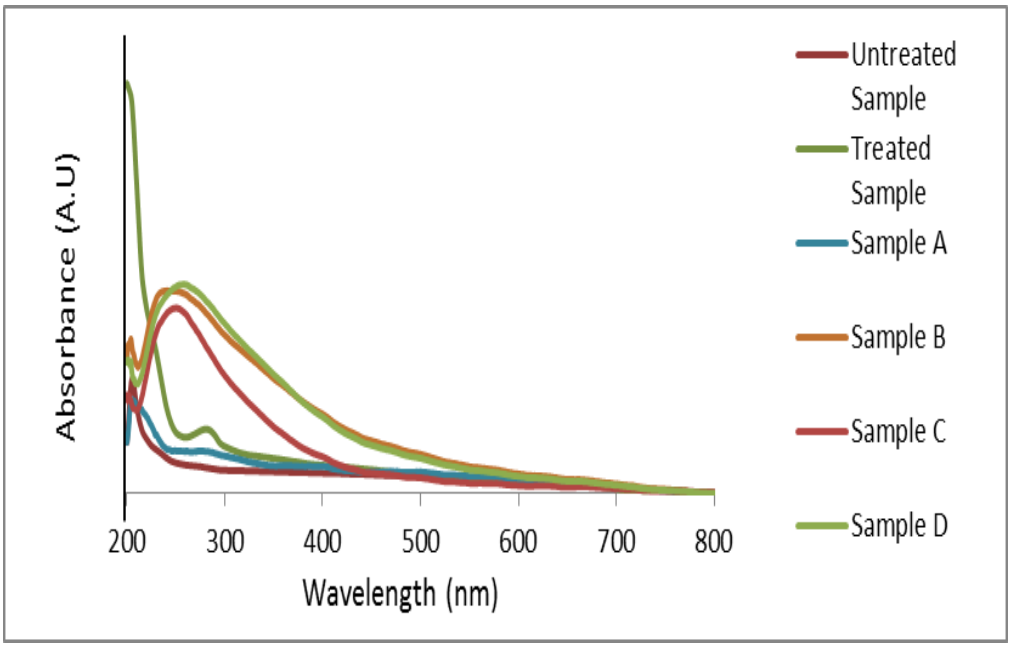

Figure 4.9 : UV-Vis absorption spectra for all samples at room temperature.

Figure 4.9 shows the absorption spectra for all samples. The absorption peaks are shifted to the larger wavelength after samples are purified and gradually added with Cu_2O. Table 4.2 summarized the results. This indicates that the diameter of α-CNT is increased with the addition of Cu_2O. These results are completely in a good agreement with the FE-SEM and TEM results.

Table 4.2: Wavelength for all samples at room temperature.

Sample	Absorption wavelength (nm)	Estimated optical band gap from Tauc/ Davis-Mott Plot (eV)
Untreated	205	5.25
Treated	210	4.7
A	220	4.65
B	230	4.6
C	240	4.55
D	250	4.5

The index value n = 1/2 is selected to obtain the suitable Tauc/Davis-Mott plots. E_g of the samples are estimated in Figure 4.10 and summarized in Table 4.2. It is interesting that E_g for α-CNTs are higher than that of the hybridized CNTs. The quantum confinement effect leads to the higher value of Eg. The value of Eg is decreased with addition of the amount of Cu_2O.

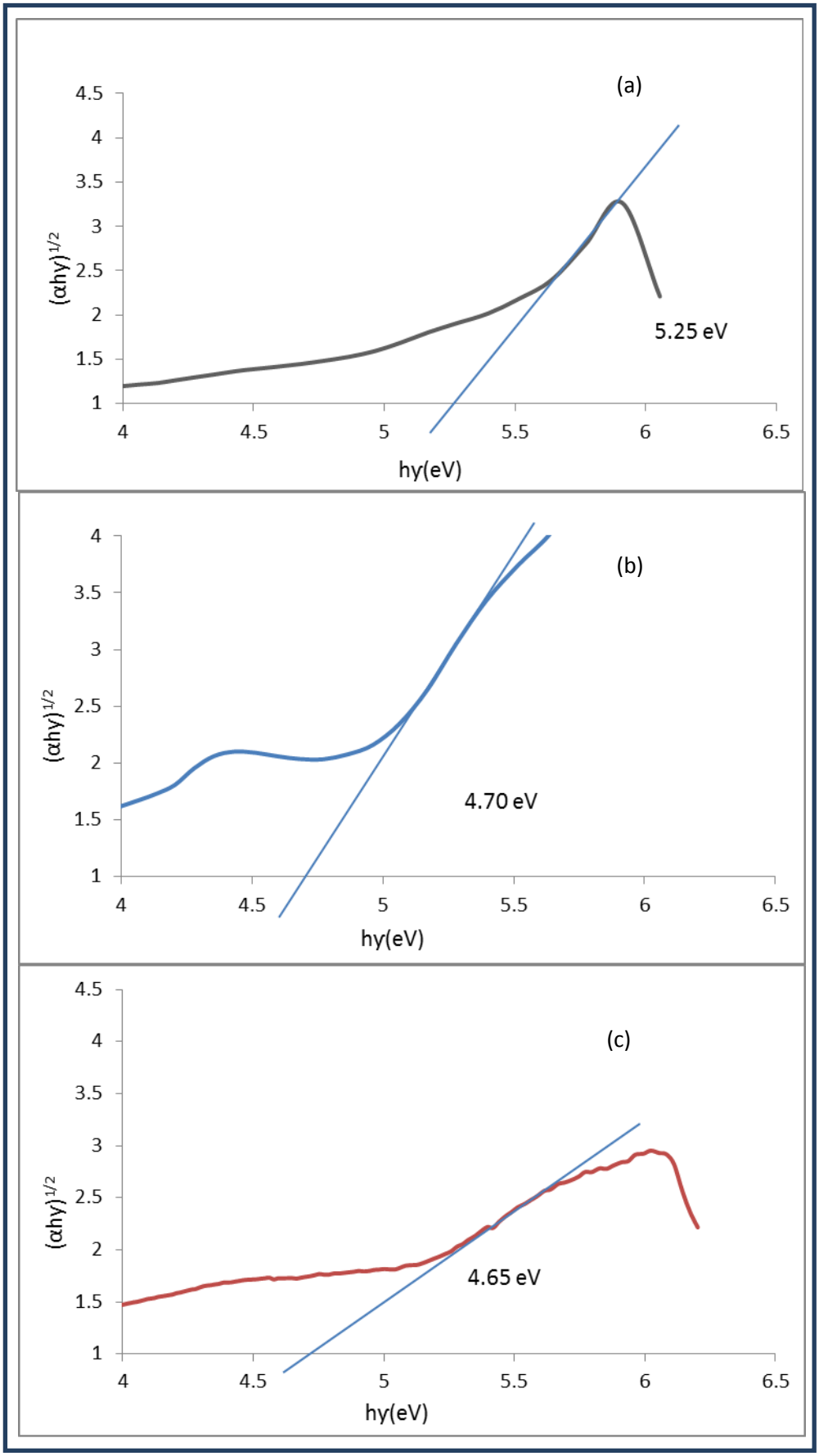
(a)
4.5
4
3.5
3
2.5
2
1.5
1
(αhy)^1/2
5.25 eV
4
4.5
5
5.5
6
6.5
hy(eV)
(b)
4
3.5
3
2.5
2
1.5
1
(αhy)^1/2
4.70 eV
4
4.5
5
5.5
6
6.5
hy(eV)
(c)
4.5
4
3.5
3
2.5
2
1.5
1
(αhy)^1/2
4.65 eV
4
4.5
5
5.5
6
6.5
hy(eV)

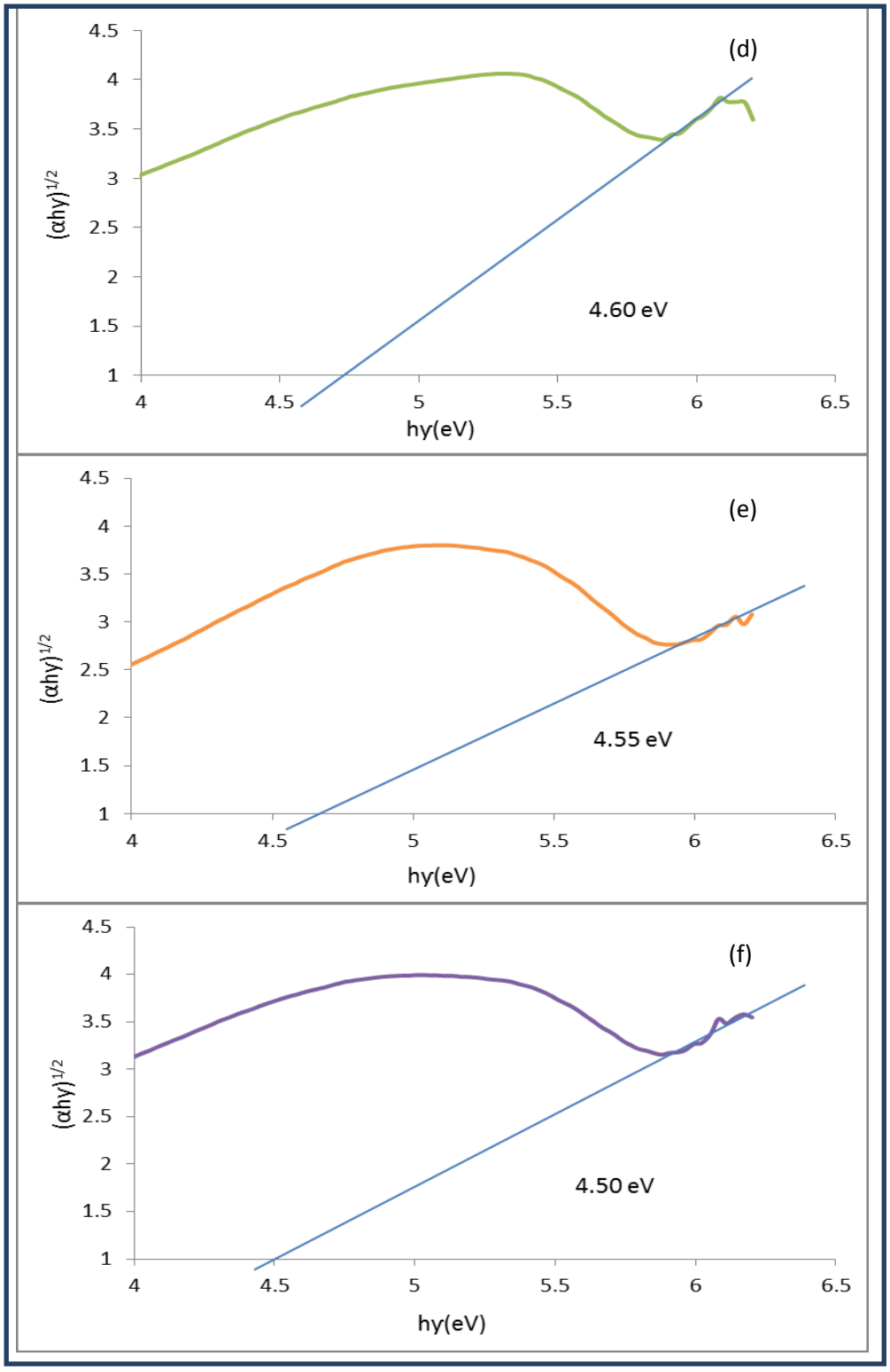

Figure 4.10: Tauc/Davis-Mott plots for $(\alpha h\gamma)^{1/2}$ as a function of hγ for all samples: (a)Untreated sample; (b) Treated sample; (c) Sample A; (d) Sample B; (e) Sample C; (f) Sample D.

Figure 4.11 shows the transmittance spectra for all samples. Overall, the transmittance hybridizedsample from A to D have remained well dispersed in the solution with a stable dispersion characteristic. It is because, the surfaces of nanotubes have been modified chemically by the hybridization treatment with copper oxide and thus results in a dramatic reduction of agglomeration effect.

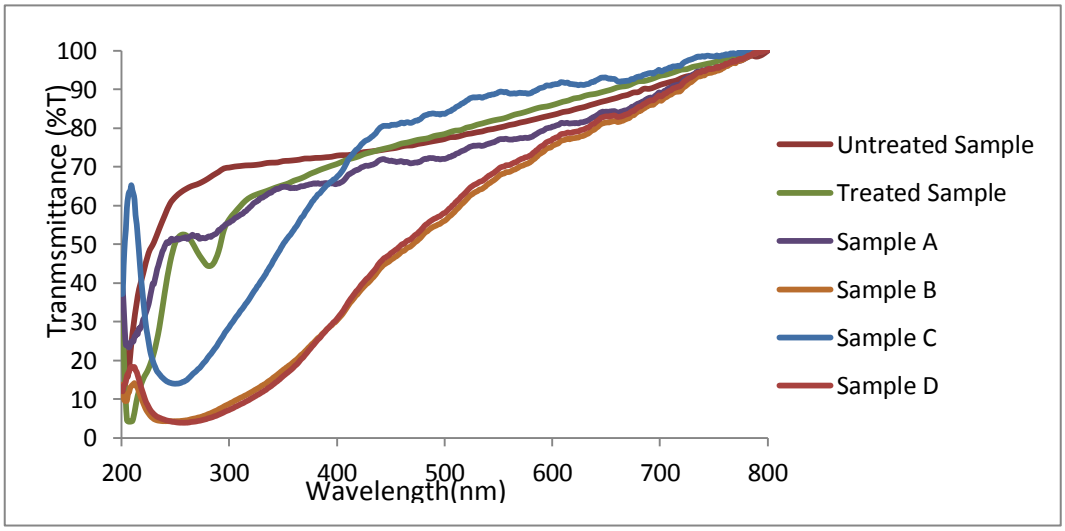

Figure 4.11 : UV-Vis transmittance spectra for all samples at room temperature.

4.4.2 Raman Spectroscopy Studies

Figures 4.12 – 4.14 show the Raman spectra for the treated and hybrid samples.

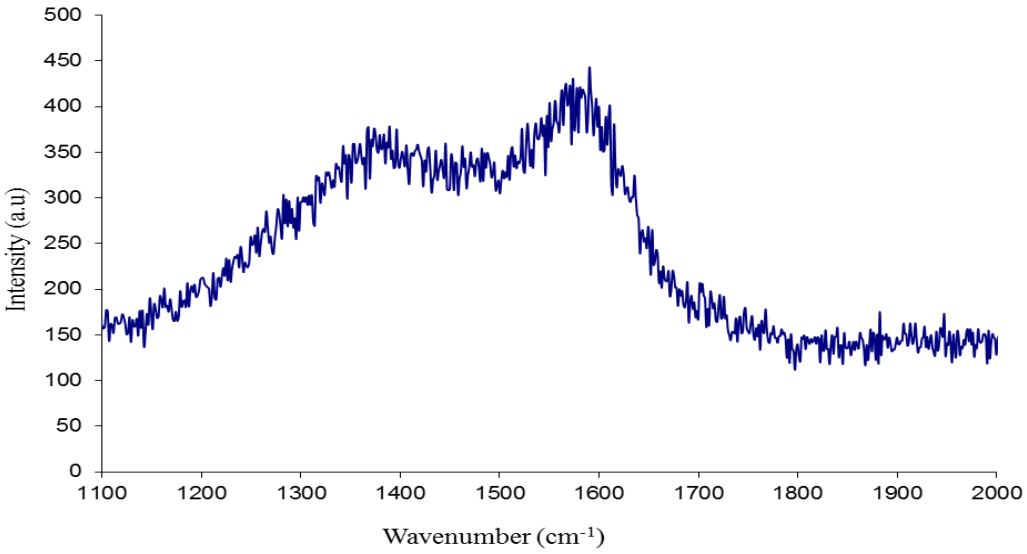

Figure 4.12: Raman spectra for treated sample at room temperature.

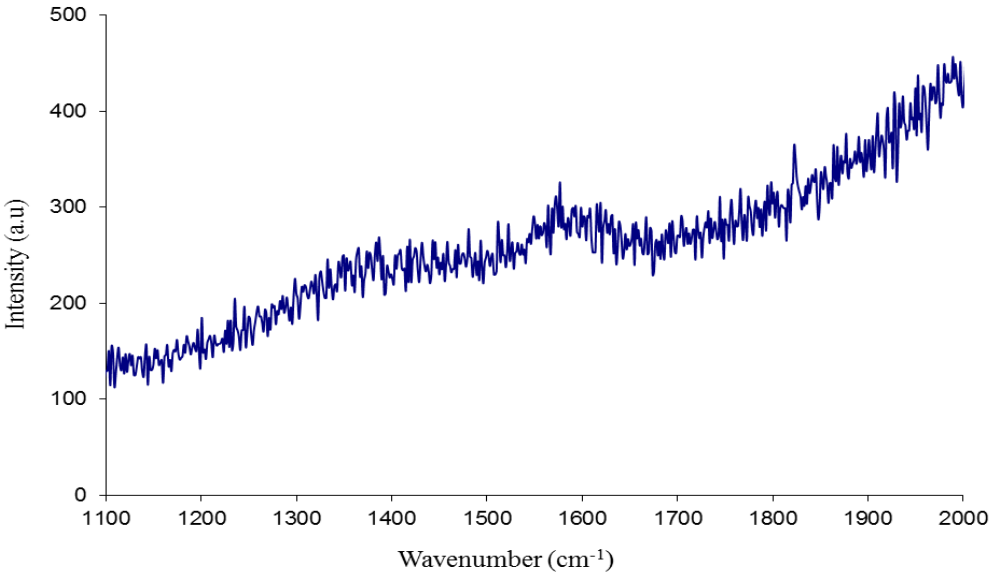

Figure 4.13: Raman spectra for hybrid sample with 0.2 g of Cu_2O at room temperature.

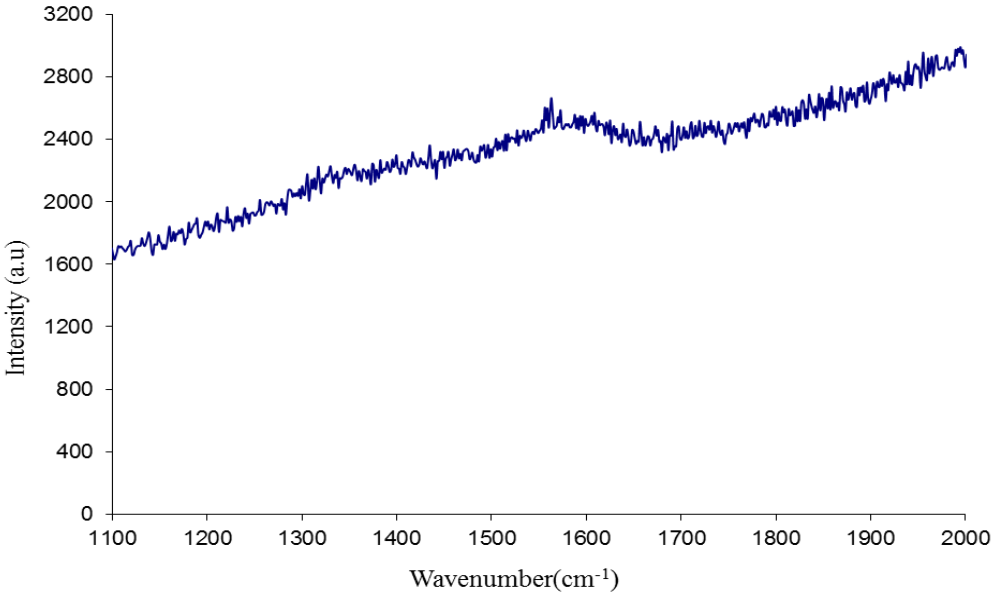

Figure 4.14: Raman spectra for hybrid sample with 1.0 g of Cu_2O at room temperature.

The Raman spectra show in the figures 4.8 – 4.10 above exhibits two peaks which correspond to the D and G bands of graphite. These are the characteristics of CNTs vibration mode. The D band appears at 1350 cm^{-1} for treated sample, 1380 $cm^{-1}$and 1325 cm^{-1} for hybrid samples with lower and higher amount of Cu_2O, respectively. The D band attributed to the Raman- inactive A_{1g} in-plane breathing vibration mode. It can be assigned to the vibrations of carbon atoms with dangling bonds in plane terminations of disordered graphite and thus being associated with the presence of defects within the hexagonal graphite layers (Cheng *et al*, 2006). The G band appears at 1584 cm^{-1} for treated sample, 1540 cm^{-1} and 1550 cm^{-1} for hybrid samples with the lower and higher amount of Cu_2O,respectively. G band attributed to the Raman-active E_{2g} in-plane vibration mode which are related to the vibration of sp^2 bonding within the carbon atoms in a two dimensional hexagonal lattice, such as in a graphite layer. As can be seen from the result, the intensity of the doublet peak for all samples increased after certain amount

of Cu_2O being added. When 1.0 g of Cu_2O is added, the intensity of the G-band of Raman spectrum increased in comparison with that at 0.2 g if Cu_2O. Such a variation can also be verified by the XRD results (Figure 4.7).

CHAPTER FIVE

CONCLUSION

The whole research presents an insight on the effect of hybridizing amorphous carbon nanotubes (α-CNTs) with Cu_2O. This research has been conducted due to the fact that little has been known about hybridize Cu_2O with α-CNTs. Therefore, the main of this study is to observe the ability of Cu_2O hybridized with α-CNTs. In general, all of the objectives are achieved.

Morphological studies have been conducted by using characterization methods like FE-SEM and TEM. The following results can be drawn from the morphological studies results:

i. The nanotubes in the untreated samples have rough surfaces and are bound in bundles disorderly.
ii. The tubular structure of nanotubes with open ends become visible in the treated sample.
iii. The surface of the nanotubes has become smooth after undergoing purification process.
iv. Increasing diameter of the nanotubes after being coated with Cu_2O.
v. The attachment of Cu_2O at the surfaces of nanotubes is confirmed.

It has been noticed that the morphological of the nanotubes after hybridization is changed. Therefore, it could be concluded that the α-CNTs were successfully hybridized by Cu_2O.

Besides, from morphological studies, it also can be concluded that band gap for hybridized sample is higher than the untreated and treated sample.

In Raman spectra, two identical bands which correspond to the D and G bands of graphite for characterizing CNTs are present.

From above, we understand that Cu_2O is definitely a suitable material to be considered and further properties studies could be developed from here, and the α-CNTs can be transferred into crystalline CNT by doing heating treatment at higher temperature.

Besides from morphological studies, it also can be concluded that The optical band gap (E_g) for hybrized sample is higher than the untreated and treated sample.

In Raman spectra, two identical bands which correspond to the D and G bands of graphite for characterizing CNTs are present.

From above, we understand that Cu_2O is definitely a suitable material to be considered and further properties studies could be developed from here.

REFERENCES

A.E. Rakshani (1986). Solid-State Electron.29, 7.

Ahmed, Sk. F., Mitra, M. K., &Chattopadhya, K. K. (2007a).Low-macroscopic field emission from silicon-incorporated diamond-like carbon film synthesized by dc PECV.*Applied Surface Science*, 253(12) 5480-5484.

Ahmed, Sk. F., Mitra, M. K., &Chattopadhya, K. K. (2007b).The effect of fluorine doping and temperature on the field emission from diamond-like carbon films.*Journal of Physic: Condensed Matter*,19(34), 346233-346247.

A. Jha, D. Banerjee, K.K. Chattopadhyyay.(2009) Low-temperature synthesis of amorphous carbon nanoneedle and study on its field emission property. *Physica E 41*, 1174-78.

Ali Can Zaman, Cem B. Ustundag, Ali Celik, Alpagut Kara, Figen Kaya, Cengiz Kaya (2010). Carbon nanotube/boehmite-derived alumina ceramics obtained by hydrothermal synthesis and spark plasma sintering (SPS). *Journal of the European Ceramic Society 30*, 3351-56.

B. Balamurunga, B.R. Mehta (2001). Thin Solid Films 396, 90.

Bethune, D. S., Kiang, C. H., de Vries, M. S., Gorman, G., Savoy, R., Vazquez, J., &Bayers, R.(1993). Cobalt-Catalysed Growth of Carbon Nanotubes with Single-Atomic-Layer Walls.*Nature*, 363, 605-607.

Byrappa,K., &Adschiri, T. (2007).Hydrothermal technology for nanotechnology.*Progress in Crystal Growth and Characterization of Materials*,53(2), 117-166.

Chik, H., &Xu, J. M. (2004).Nanometricsuperlattices: non-lithographic fabrication, materials, and prospects. *Materials Science and Engineering: R: Reports*, 43(4), 103-138.

Ci, Lijie, Wei, Bingqing, Xu, Cailu, Liang, Ji, Wu, Dehai, Xie, Sishen, Zhou, Weiya, Li, Yubao, Liu, Zuqin, & Tang, Dongsheng. (2001). Crystallization behavior of the amorphous carbon nanotubes prepared by the CVD method.*Journal of Crystal Growth*, 233(4), 823-828.

Ci, Lijie, Zhu, Hongwei, Wei, Bingqing, Xu, Cailu, & Wu, Dehai. (2003). Annealing amorphous carbon nanotubes for their application in hydrogen storage. *Applied Surface Science*, 205(1-4), 39-43.

CmarOncel and YudaYurum (2004). Carbon Nanotube Synthesis via the Catalytic CVD Method: A Review on the effect of Reaction Parameters.

D.S. Kim, T. Lee, K.E. Geckeler, Angew. Chem. Int. Ed. 45 (2006) 104.

Dresselhaus, M. S., Dresselhaus, G., Jorio, A., Souza Filho, A. G., & Saito, R. (2002). Raman spectroscopy on isolated single wall carbon nanotubes.*Carbon*, 40(12), 2043-2061.

E.A. Souza, R. Landers, L.P. Cardoso, T.G.S. Cruz, M.H. Tabackniks, A. Gorenstein (2006). *Journal of Power Sources* 155,358–363.

Ebbesen, T. W., & Ajayan, P. M. (1992). Large-scale synthesis of carbon nanotubes. *Nature*, 358, 220-222.

E. Dominik (2010). Carbonnanotubes-inorganic hybrids, *Chem.Rev*, 110, 1348-85

Gojny, FH., Nastalczyk, J., Roslaniec, Z., & Schulte, K (2003). Surface modified multi-walled carbon nanotubes in CNT/epoxy-composites. *Chemical Physics Letters*, 370(5-6), 820-824.

Hu G, Cheng M, Ma D, Bao XH (2003). Synthesis of carbon nanotube bundles with mesoporous structure by a self-assembly solvothermal route.*ChemMater* ; 15: 1470-3

Xiong YJ, Xie Y, Li XX, Li ZQ (2004). Production of novel amorphous carbon nanostructures from ferrocene in low-temperature solution.*Carbon*; 42; 1447-53.

Hutchison, J. L., Kiselev, N. A., Krinichnaya, E. P., Krestinin, A. V., Loutfy, R. O., Morawsky, A. P., Muradyan, V. E., Obraztsova, E. D., Sloan, J., Terekhov, S.V., & Zakharov, D.N. (2001). Double-walled carbon nanotubes fabricated by a hydrogen arc discharge method. *Carbon*, 39(5), 761-770

Iijima, S. (1991).Helical microtubules of graphitic carbon.*Nature*,354 , 56-58.

Jha, A., Banerjee, D., &Chattopadhyay, K. K. (2011).Improved field emission from amorphous carbon nanotubes by surface functionalization with stearic acid.*Carbon*,49(4),1272-1278.

J. Morales, L. Sanchez, F. Martin, J.R. Ramos-Barrado, M. Sanchez (2005).*Thin Solid Films* 474 (2005) 133–140.

J. Zhu, M. Brink, P.I. McEuen, Nano Lett. 8 (2008) 2399.

Kieran MacKenzie, Oscar Dunens, Andrew T. Harris. A review of carbon nanotube purification by microwave assisted acid digestion. Separation and Purification Technology 66 (2009) 209-222.

Li, W. Z., Xie, S. S., Qian, L. X., Chang, B. H., Zou, B. S., Zhou, W. Y., Zhao, R. A., & Wang, G. (1996). Large-scale synthesis of aligned carbon nanotubes.*Science*, 274(5293), 1701-1703.

Liu, Boyang, Jia, DechangJia, Zhou, Yu, Feng, Haibo, &Meng, Qingchang. (2007). Low temperature synthesis of amorphous carbon nanotubes in air. *Carbon*, 45(8), 1710-1713.

Liu, YN, Song, XL, Zhao, TK, Zhu, JW, Hirscher, M, & Philipp, F. (2004). Amorphous carbon nanotubes produced by a temperature controlled DC arc discharge. *Carbon*, 42(8-9), 1852-1855.

Luo, Tao, Chen, Luyang, Bao, Keyan, Yu, Weichao, &Qian, Yitai. (2006). Solvothermal preparation of amorphous carbon nanotubes and Fe/C coaxial nanocables from sulfur, ferrocene, and benzene.*Carbon*, 44(13), 2844-2848.

Melissa Paradise &TarunGoswami.(2007). Carbon nanotubes - Production and industrial applications.*Materials & Design*, 28(5), 1477-1489.

Meyyappan, M. (2005).Carbon nanotubes science and applications.*Boca Raton*: CRC Press LLC

Nishino H, Nishida R, Matsui T, Kawase N, Mochida I (2003). Growth of amorphous carbon nanotube from poly(tetrafluoroethylene) and ferrous chloride. *Carbon*; 41 (14): 2819-23.

Nishino H, Yamaguchi C, Nakaoka H, Nishida R (2003). Carbon nanotube with amorphous carbon wall: α-CNT. *Carbon*; 41(11): 2165-7.

O'Connell, M. J. (2006). Carbon nanotubes properties and applications.*Boca Raton*: CRC Press

Peter, J. F. H. (2009). Carbon nanotube science: Synthesis, properties and applications. New York: *Cambridge University Press*.

P.M. Ajayan (1999). Chemical Reviews, *Vol. 99*, 1787.

RajendraSrivastava, M.U. AnuPrathap, RajkumarKore. Morphologically controlled synthesis of copper oxides and their catalytic applications in the synthesis of propargylamine and oxidative degradation of methylene blue. (2011). Colloids and Surfaces A: Physicochemical and Engineering Aspects.271-282.

Rakitin, A., Papadopoulos, C., & Xu, JM. (2000). Electronic properties of amorphous carbon
nanotubes. *Physical Review B*, 61(8), 5793-5796.

Ren, Z. F., Huang, Z. P., Xu, J. W., Wang, J. H., Bush, P., Siegal, M. P., &Provencio, P. N. (1998). Synthesis of large arrays of well-aligned carbon nanotubes on glass.*Science, 282*(5391), 1105-1107.

Saito, R., Dresselhaus, G., & Dresselhaus, M. S. (Eds.). (1988). Physical properties of carbon nanotubes. London: *Imperial College Press*.

Saito, Y., &Uemura, S. (2000). Field emission from carbon nanotubes and its application to electron sources.*Carbon*, 38(2), 169-182.

S. Ghosh, D.K. Avasthi, P. Shah, V. Ganesan, A. Gupta,D. Sarangi, R. Bhattacharya, W. Assmann,(2000). Vacuum 57.377–385.

Speck, S., Endo, M., &Dresselhaus, M. S. (1989). Structure and intercalation of thin benzene derived carbon fibers. *Journal of Crystal Growth*, *94*(4), 834-848.

.

Sui, Y. C., Acosta, D. R., González-León, J. A., Bermúdez, A., Feuchtwanger, J., Cui, B. Z., Flores, J. O., &Saniger, J. M. (2001). Structure, thermal stability, and deformation of multibranched carbon nanotubes synthesized by CVD in the AAO template.*Journal of Physical Chemistry B*, *105*(8), 1523-1527

Takeshi Akasaka, Fred Wudl, Shigeru Nagase (2010). Chemistry of Nanocarbons, *Wiley.*

Tingkai Zhao, Yongning Liu, Jiewu Zhu (2005). Temperature and catalyst effects on the production of amorphous carbon nanotubes by a modified arc discharge. *Carbon 43*,2907-2912.

Vikas Mittal (2010).Polymer nanotube nanocomposites, synthesis, properties, and applications.

Wang, W. Z., Huang, J. Y., Wang, D. Z., &Ren, Z. F. (2005b).Low-temperature hydrothermal synthesis of multiwall carbon nanotubes.*Carbon*, 43(6), 1328-1331.

Wang, W. Z., Poudel, B., Wang, D. Z., &Ren, Z.F. (2005a).*Synthesis of multiwalled carbon nanotubes through a modified Wolff-Kishner reduction process*. Journal of the American Chemical Society, 127(51), 18018-18019.

Wang, X., Li, Q., Xie, J., Jin, Z., Wang, J., Li, Y., Jiang, K., & Fan, S. (2009). Fabrication of ultralong and electrically uniform single-walled carbon nanotubes on clean substrates.*Nano Letters*, 9(9), 3137-3141.

Wang, Xizhang, Hu, Zheng, Wu, Qiang, & Chen, Yi. (2002). Low-temperature catalytic growth of carbon nanotubes under microwave plasma assistance.*Catalysis Today*, 72(3-4), 205-211.

Xiong, Yujie, Xie, Yi, Li, Xiaoxu, & Li, Zhengquan. (2004). Production of novel amorphous carbon nanostructures from ferrocene in low-temperature solution.*Carbon*, 42(8-9), 1447-1453.

Yang, Y., Hu, Z., Wu, Q., Lü, Y. N., Wang, X. Z., & Chen, Y. (2003). Template-confined growth and structural characterization of amorphous carbon nanotubes.*Chemical Physics Letters*, 373(5-6), 580-585.

Zhao, N.H., Zhang, P., Yang, L.C., Fu, L. J., Wang, B., & Wu, Y. P. (2009). Tunable amorphous carbon nanotubes prepared by a simple template. *Materials Letters*, 63(22), 1955-1957.

Zhao, N. Q., He, C. N., Du, X. W., Shi, C. S., Li, J. J., & Cui, L. (2006). Amorphous carbon nanotubes fabricated by low-temperature chemical vapor deposition. *Carbon*, 44(9), 1859-1862.